

CONFIDENTIAL

436

Copy
RM E53H15

NACA RM E53H15

CASE FILE
COPY NACA

RESEARCH MEMORANDUM

EFFECT OF FLAME-HOLDER DESIGN ON ALTITUDE PERFORMANCE

OF LOUVERED-LINER AFTERBURNER

By Paul E. Renas and Emmert T. Jansen

Lewis Flight Propulsion Laboratory
Cleveland, Ohio

CLASSIFICATION CHANGED TO UNCLASSIFIED
AUTHORITY: NASA TECHNICAL PUBLICATIONS
ANNOUNCEMENTS NO. 45
EFFECTIVE DATE: APRIL 12, 1961
WHL

CLASSIFIED DOCUMENT

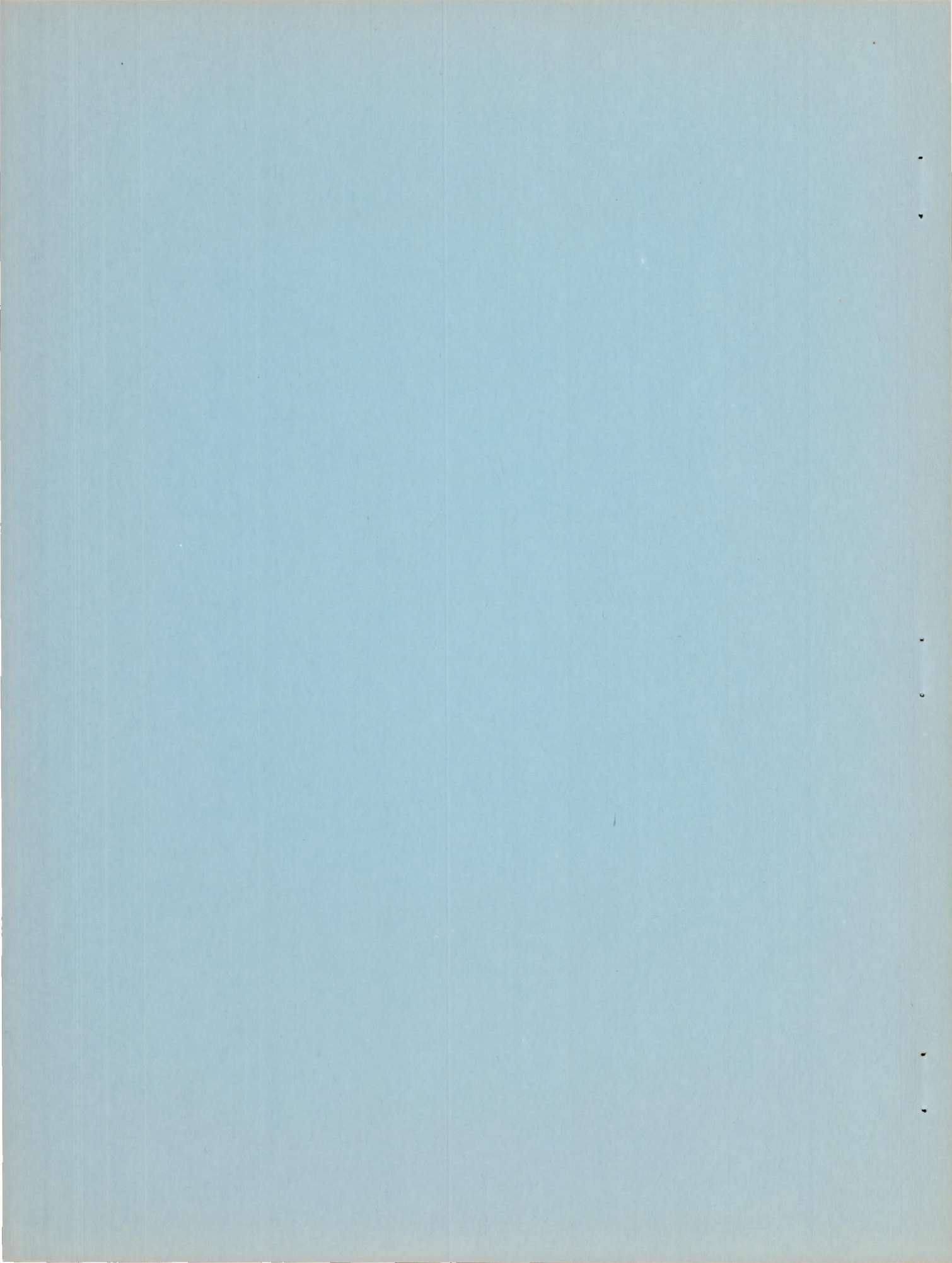
This material contains information affecting the National Defense of the United States within the meaning of the espionage laws, Title 18, U.S.C., Secs. 793 and 794, the transmission or revelation of which in any manner to an unauthorized person is prohibited by law.

NATIONAL ADVISORY COMMITTEE
FOR AERONAUTICS

WASHINGTON

October 9, 1958

CONFIDENTIAL



NATIONAL ADVISORY COMMITTEE FOR AERONAUTICS

RESEARCH MEMORANDUM

EFFECT OF FLAME-HOLDER DESIGN ON ALTITUDE PERFORMANCE

OF LOUVERED-LINER AFTERBURNER

By Paul E. Renas and Emmert T. Jansen

SUMMARY

An investigation was conducted in an altitude test chamber to determine criteria for the design of flame holders for a turbojet-engine afterburner. The performance of ten flame holders was obtained in a louvered-liner afterburner operated at constant afterburner-inlet temperature over a range of fuel-air ratio at afterburner-inlet total pressures of 1125 and 680 pounds per square foot. The performance of one of the better flame holders was obtained over a range of afterburner fuel-air ratio at afterburner-inlet total pressures ranging from 3130 to 680 pounds per square foot.

A V-gutter flame holder had consistently higher combustion efficiency and altitude operating limits than a U-gutter flame holder. Adding louvers to the U-gutter did not completely eliminate the difference in combustion efficiency between the two flame holders, but did overcome the difference in altitude operating limits. The data showed no marked superiority of either a 2- or a $1\frac{1}{2}$ -inch-wide gutter. However, proper gutter width must be accompanied by proper radial positioning of the gutters with respect to the velocity profile in order to ensure satisfactory performance. Increasing the blocked area from 22.3 to 30.8 percent resulted in substantial improvement in combustion efficiency, while using interconnecting gutters between the rings improved the altitude operational characteristics of the afterburner without loss in performance at the higher pressure levels.

INTRODUCTION

Previous research investigations related to afterburners for full-scale turbojet engines, such as reported in references 1 to 4, have usually had as their primary objective the development of a satisfactory afterburner to meet certain performance specifications for the particular

engines. Because this objective was paramount and the time available for the studies was limited, these investigations did not permit configuration changes to be made with systematic variations of individual components. An additional reason for the difficulty in obtaining systematic design information is that the components of an afterburner, such as the diffuser, the fuel system, and the flame holder, have interrelated effects on afterburner performance, so that results obtained by varying one component at a time are sometimes applicable only to the particular configuration being investigated.

It has been determined, however, from numerous investigations that, if the flame-holder inlet velocity profile is typical and the fuel-air-ratio profile is reasonably uniform, a favorable environment is provided, so that changing the flame holder alone may provide significant design information. Even with typical velocity and uniform fuel-air ratio profiles, data obtained from any investigation are limited by the particular environment. The present investigation was made with an afterburner typical of current practice, having reasonable flame-holder inlet gas velocities, fairly high turbine-outlet gas temperatures, a spray-bar fuel system, reasonable fuel-mixing length, and, in addition, a louvered cooling liner. Therefore, the results presented herein are applicable to typical afterburners with louvered cooling liners.

A fairly uniform fuel-air-ratio profile at the flame-holder inlet having previously been established for the particular afterburner used in this investigation, flame-holder designs were varied while all other components of the afterburner remained unchanged. Ten flame holders were investigated, which differed in gutter cross-sectional shape, gutter width, radial location of gutters, blocked area, and the addition of a trailing V-gutter and interconnecting V-gutters to a V-gutter flame holder. The data presented for the various configurations show the effects of flame-holder design on performance at afterburner-inlet total pressures of 1125 and 680 pounds per square foot. Along with the steady-state performance, the altitude operational limits are presented for each flame holder.

APPARATUS

Engine and Afterburner

The turbojet engine and afterburner used in this investigation are shown in figure 1. The engine has a guaranteed static sea-level dry thrust rating of 5425 pounds at a rated engine speed of 7950 rpm and a rated turbine-outlet "control" temperature of 1300° F. The main components of the engine include a 12-stage axial-flow compressor, eight can-type combustion chambers, and a single-stage turbine. The components of the afterburner are a diffuser, a fuel injection system, a flame holder, a combustion chamber, a clamshell-type variable-area exhaust

nozzle, and an integrated electronic control. The length of the diffuser is $45\frac{3}{4}$ inches, while the over-all length of the afterburner (including diffuser) is approximately 100 inches. The flame holders were mounted on a rod extending from the aft end of the diffuser inner body, as shown in figures 2 and 3.

The afterburner fuel injection system was made up of 20 fuel-spray bars (each having 19 fuel orifices) equally spaced circumferentially and located 27 inches downstream of the turbine outlet (fig. 2) and approximately 22 inches upstream of the flame holder. The individual fuel orifices (all 0.020-in. diam.) injected fuel normal to the gas stream, except for one orifice near the tip of each bar that injected fuel upstream.

Cooling of the afterburner shell was accomplished by the use of a louvered liner (fig. 4) that extended from about 1 inch downstream of the fuel-spray bars to within $1/2$ inch of the fixed portion of the exhaust-nozzle outlet. The height of this cooling passage varied from approximately $1\frac{1}{4}$ inches at the inlet to $1/2$ inch at the outlet. A mixture of air and combustion gases entered the cooling passage at turbine-outlet temperature and was fed back into the primary combustion zone through louvers along the entire length of the combustion chamber.

The clamshell-type variable-area exhaust nozzle, which was actuated by the integrating electronic control, maintained constant turbine-outlet temperature over the entire operable range of afterburner fuel flow. The projected area variation of the exhaust nozzle was from 257 to 452 square inches. Throughout the investigation, MIL-F-5624A, grade JP-4, fuel was used in both the engine and the afterburner.

Altitude Chamber

The engine with afterburner was installed in an altitude test chamber 10 feet in diameter and 60 feet long. The engine was mounted on a thrust-measuring bed hung from four pendulum-type supports with flexure plates at each end. The thrust force was transmitted through a bell crank and lever system to a null-type force-measuring cell. A front bulkhead, which incorporated a labyrinth seal around the forward end of the engine, separated the engine and exhaust sections of the chamber and allowed freedom of movement of the engine in an axial direction. A rear bulkhead was installed just ahead of the nozzle exit to act as a radiation shield and to prevent recirculation of the hot exhaust gases around the engine.

Instrumentation

The location of instrumentation at the stations before and after each of the principal components of the engine and the afterburner is shown in figure 1. The air flow was determined from pressure and temperature measurements at the engine inlet and corrected for any known leakage or cooling-air flow. The pressures at the exhaust nozzle were measured with a water-cooled rake, and the fuel flows to the engine and the afterburner were measured independently with calibrated rotameters.

Flame Holders

A detailed description of each flame holder is presented in table I, and sketches and photographs are shown in figure 5. The percentage of blocked area for each flame holder is based on the ratio of flame-holding area to total cross-sectional area of the outer shell at the location of the flame holder (5.68 sq ft). (The cross-sectional area of the cooling liner at the flame-holder location is 4.84 sq ft.)

The flame-holder design variables investigated include gutter cross-sectional shape, gutter width, radial location of gutters, blocked area, and the addition of a trailing V-gutter and interconnecting V-gutters to a 2-ring V-gutter flame holder. The flame holders associated with each of the design variables are listed in the following table:

Design variable	Flame holder
Gutter cross-sectional shape	1, 2, 3, 4
Gutter width and radial location of gutters	5, 6, 7, 8, 9
Flame-holder blocked area	1, 5, 6, 7, 9
Modifications to 2-ring V-gutter	1, 5, 10

PROCEDURE

For each flame holder, performance data were obtained at an afterburner-inlet temperature of 1810° R ($\pm 25^\circ$) and afterburner-inlet total pressures of 1125 and 680 pounds per square foot, which correspond to simulated flight conditions at 40,000 and 50,000 feet at a Mach number of 0.60. The maximum altitude operating limit was also determined for each flame holder, but for some configurations this altitude operating

limit was lower than 50,000, or even lower than 40,000 feet. One of the more satisfactory configurations was run over a range of afterburner-inlet total pressure from 3130 to 680 pounds per square foot, corresponding to operation at altitudes from 15,000 to 50,000 feet at a flight Mach number of 0.60.

The simulated flight condition was obtained by setting the engine-inlet temperature and total pressure and the exhaust static pressure to the desired NACA standard altitude conditions with the assumption of 100-percent free-stream ram-pressure recovery. At each flight condition with the engine operating at rated speed, data were obtained over a range of afterburner fuel-air ratio that was limited by lean blow-out at one end and maximum exhaust-nozzle area or maximum thrust at the other. The fuel-air ratio is the ratio of afterburner fuel plus unburned engine fuel to unburned air entering the afterburner. In order to determine the maximum altitude operating limit, the afterburner was operated at approximately constant fuel-air ratio while the altitude was increased at constant flight Mach number until afterburner blow-out occurred. The methods of calculations of the performance along with the symbols are presented in the appendix.

RESULTS AND DISCUSSION

During a full-scale flame-holder investigation, it is generally impossible to vary one specific design variable of a flame holder and hold all other variables constant. For example, changing the flame-holder blocked area with a constant afterburner cross-sectional area necessitates altering either the gutter width, the gutter diameter, or the number of gutter rings. Wherever possible, these secondary changes were kept to a minimum.

Sample velocity and fuel-air-ratio profiles at the flame-holder inlet for the afterburner used in this investigation are presented in figure 6. The velocity of the gases at the flame-holder inlet vary from about 540 feet per second at the outer shell to 300 feet per second near the surface of the diffuser inner body. This velocity profile is not ideal, but it is typical of the velocity distribution for a reasonably good diffuser design. Therefore, the matching problems encountered between the velocity profile and the flame holder are also typical. The fuel injection system, which was tailored to match the air-flow profile at the point of fuel injection in order to provide a uniform fuel-air-ratio profile at the flame-holder inlet, was maintained constant throughout the flame-holder investigation. Because the fuel-air-ratio is approximately uniform across the combustion chamber, the problem of matching the radial flame-holding-area location to the fuel-air-mixture profile was minimized.

The performance parameters presented for the various flame-holder configurations investigated are afterburner total-pressure loss ratio, afterburner combustion efficiency, and augmented net thrust ratio. Accompanying these performance comparisons are the operational characteristics for the configurations, showing the lean blow-out limits, the rich limits, and the maximum altitude operating limits.

Effect of Gutter Cross-Sectional Shape

Afterburner performance and operational limits for flame holders with various gutter cross-sectional shapes are shown in figures 7 and 8. The flame holders used for the comparison include a V-gutter, a closed V-gutter, a U-gutter, and a U-gutter with louvers (flame holders 1, 2, 3, and 4, respectively). Each flame holder has a blocked area of about $22\frac{1}{4}$ percent, and the effect of slight variations in gutter diameter on performance are believed to be negligible.

For a given fuel-air ratio, within the range that the data may be compared, the afterburner total-pressure loss ratio for the U-gutter flame holder was about 0.02 less than that for the V-gutter or for the closed V-gutter (fig. 7). However, associated with this lower pressure loss are a lower combustion efficiency and a lower augmented net thrust ratio. At an afterburner-inlet total pressure of 1125 pounds per square foot, the maximum combustion efficiencies occurred at a fuel-air ratio of 0.04 and were 0.73, 0.63, 0.60, and 0.54 for the closed V-gutter, the V-gutter, the U-gutter, and the U-gutter with louvers, respectively. The improved performance at this pressure level of the closed V-gutter over the conventional V-gutter is attributed to the high surface temperature of the aft portion of the closed V-gutter. At an afterburner-inlet total pressure of 680 pounds per square foot the maximum combustion efficiency occurred at a fuel-air ratio of about 0.05 and was 0.55 for both the V-gutter and closed V-gutter; while the maximum combustion efficiencies for the U-gutter and the U-gutter with louvers were 8 and 12 points lower, respectively. It was observed that the aft portion of the closed V-gutter did not reach as high a surface temperature at this low pressure as at 1125 pounds per square foot. The relatively small differences between the two types of flame holder at the low pressure level are therefore attributed to the absence of the favorable effects of the hot gutter surface.

The relatively low combustion efficiencies shown in figure 7, along with the low efficiencies for all data presented herein, are characteristic of this louvered-cooling-liner afterburner. Instrumentation at four stations spaced approximately equally along the length of the liner indicated cooling-gas flows of 24, 20, 16, and 5 percent of the turbine-outlet gas flow. This large quantity of cooling gas, which

is bled back into the combustion chamber, apparently dilutes the fuel-air mixture, quenches the flame in the outer region of the primary combustion zone, and thereby causes a decrease in combustion efficiency. Comparing the performance of the afterburner used in this investigation with the performance of a similar afterburner on the same engine but without a cooling liner, showed a reduction in combustion efficiency of between 10 and 20 points due to the addition of the cooling liner. Because the effect of this cooling-gas flow on the comparison of various flame holders is unknown, the results of this investigation may not be generally applicable to afterburners without similar cooling liners.

The effect of adding louvers to the leading edge of a U-gutter is shown by a comparison of the performance of flame holders 3 and 4. Blocking the louvers of flame holder 4 to form flame holder 3 increased the combustion efficiency 2 to 3 points at a pressure level of 1125 pounds per square foot, decreased the combustion efficiency 6 to 12 points at a pressure level of 680 pounds per square foot (fig. 7), and decreased the altitude limit (fig. 8) from 59,000 to 52,000 feet. The effect of the louvers on altitude limit as obtained during the present investigation is different from the trends obtained in reference 2. However, the configurations investigated in reference 2 had a fuel system comprised of rings located in most cases less than 2 inches upstream of the leading edge of the flame holder. This close spacing of the fuel injection system would tend to make the fuel-air mixture that was being bled into the flame-holding area overrich and thereby cause rich blow-out to occur at lower altitudes. With the configurations reported herein, the fuel mixing length of 22 inches allowed the fuel to atomize, vaporize, and mix with the air before being bled into the combustion zone. The bleeding of a highly combustible mixture into the sheltered primary zone of the flame holder apparently intensified the combustion and, thus, slightly improved performance and operating limits for the lower-pressure operating condition.

The operating limits for the four flame holders at altitudes above 40,000 feet are presented in figure 8. The lean blow-out limit for each of the flame holders was determined for the range of altitude from 40,000 feet to the point of intersection of the lean blow-out limit with the maximum limit of the afterburner. The maximum limit of the afterburner was determined either by full-open exhaust nozzle or maximum thrust, depending upon which occurred first as the afterburner fuel-air ratio was increased. Rich blow-out was not encountered at the pressure levels of 1125 and 680 pounds per square foot for any of the flame holders investigated. In order to obtain consistent data for altitude operating limits, similar techniques were employed in manipulating the test facility valves; and above an altitude of 50,000 feet each data point on the curve represents a minimum of two determinations of the lean blow-out limit. The maximum altitude operating limit of the U-gutter flame holder with louvers was 59,000 feet, while the

V-gutter, the closed V-gutter, and the U-gutter flame holders had altitude limits of 57,500, 55,000, and 52,000 feet, respectively. For the first three flame holders, there was little variation in the lean blow-out limit; but the U-gutter flame holder with louvers has a considerably higher lean blow-out limit. The shift in the rich limit is, in general, merely a reflection of the change in combustion efficiency and the variation in turbine-outlet temperature between configurations.

There are additional factors that must be considered when selecting the design gutter cross-sectional shape for a flame holder: the durability of the flame holder over the range of conditions to which it will be subjected, the weight, and the ease of manufacturing. Visual observations through a periscope of the closed V-gutter flame holder (gutter shape having the highest combustion efficiency) showed an overheating condition of the aft portion of the gutter rings when afterburning at a pressure of 1125 pounds per square foot. This overheating tends to indicate that the durability of the closed V-gutter flame holder at high pressure levels (low altitudes) may be poor.

Effect of Gutter Width

The radial location of the flame-holding areas and the relative size of the gutters of flame holders 1, 5, 6, 7, and 9, with respect to the velocity profile at the flame-holder inlet, are shown in figure 9. The effect of gutter width on afterburner performance and operational limits is shown in figures 10 and 11. V-gutter flame holders 5 and 9 (blocked area, about $27\frac{1}{4}$ percent; gutter widths, 2 and $1\frac{5}{8}$ in., respectively) and 6 and 7 (blocked area, about $30\frac{4}{5}$ percent; gutter widths, 2 and $1\frac{1}{2}$ in., respectively) are used for this comparison. Flame holder 8, which is a 9-ring V-gutter having a blocked area of 28 percent with $1/2$ -inch gutter widths, is also used in this comparison, but no data are shown in the figures. The secondary changes present that may affect the results are: for flame holders 5 and 9, a change in radial location of the gutters; and for flame holders 6 and 7, a change in the number of gutters and the addition of interconnecting gutters to flame holder 7.

The altitude limit of flame holder 8 ($1/2$ in. gutter widths) was slightly under 40,000 feet. The poor performance and operational characteristics were caused by the inability of the small V-gutter to provide adequate flame stabilization. Visual observation of the flame with the afterburner operating at altitude showed the fuel to be burning near the nozzle inlet and even downstream of the nozzle exit.

For a given afterburner-inlet total pressure, increasing the flame-holder blocked area increases the total-pressure loss across the afterburner; while changes in gutter width along with secondary changes to

each configuration for a given blocked area have essentially no effect on pressure loss (fig. 10). At an afterburner-inlet total pressure of 1125 pounds per square foot and for a blocked area of about $30\frac{4}{5}$ percent, decreasing the gutter width from 2 to $1\frac{1}{2}$ inches (accompanied by an increase in number of gutters from 2 to 3 and by addition of interconnecting gutters) decreased the combustion efficiency about 4 points and the augmented net thrust ratio about 2 points (fig. 10(a)). At the same pressure level, but for a blocked area of about $27\frac{1}{4}$ percent, decreasing the gutter width from 2 to $1\frac{5}{8}$ inches (accompanied by a variation in radial location of flame-holding area) increased the combustion efficiency from 2 to 10 points and the augmented net thrust ratio about 4 points. The trend of the data for both blocked areas at an afterburner-inlet total pressure of 680 pounds per square foot (fig. 10(b)) is the same as the trend at an afterburner-inlet pressure of 1125 pounds per square foot, except that the altitude limit of flame holder 6 (gutter width of 2 in. and blocked area of about $30\frac{4}{5}$ percent) was 50,000 feet (fig. 11).

If the range of operation and the altitude limit for the various flame holders are considered (fig. 11), the data indicate that the three flame holders having interconnecting gutters (5, 7, and 9) have considerably lower lean blow-out limits and also higher altitude operating limits than the flame holder without interconnecting gutters (6), irrespective of gutter width.

Thus, in the selection of the gutter width of a flame holder, the data indicate no marked superiority of either the 2- or the $1\frac{1}{2}$ -inch gutter over the other. However, decreasing the gutter width while increasing the flame-holding sources (number of gutters) will ultimately result in a drop in performance, as evidenced by the unsatisfactory performance of the nine $1\frac{1}{2}$ -inch gutters of flame holder 8. Other unpublished data indicate that $3\frac{3}{4}$ -inch gutters are also unsatisfactory. More important, (provided that the gutter width is between $1\frac{1}{2}$ and 2 in.) is the proper radial positioning of the flame-holding area with respect to the mass-flow profile and the wall surfaces of the afterburner at the flame-holder location, in order to obtain good afterburner performance.

Effect of Flame-Holder Blocked Area

Increasing the flame-holder blocked area increased the total-pressure loss across the afterburner for any given fuel-air ratio. Along with increased pressure loss with increasing blocked area is associated a general trend of increasing combustion efficiency and augmented net

thrust ratio (fig. 10). At an afterburner-inlet total pressure of 1125 pounds per square foot and for the range of fuel-air ratios investigated (fig. 10(a)), increasing the flame-holder blocked area from 22.3 to 30.8 percent increased the pressure loss about 2 points, the combustion efficiency about 15 points, and the augmented net thrust ratio about 6 points. At a pressure level of 680 pounds per square foot (fig. 10(b)), increasing the blocked area increased the pressure loss the same amount at the higher pressure level; while the increases in combustion efficiency and augmented net thrust ratio were only about 8 and $2\frac{1}{2}$ points, respectively.

From the data obtained during this investigation, the effect of flame-holder blocked area on the altitude operating limit of the afterburner is not conclusive. The altitude limit of the larger-blocked-area flame-holder configurations was lower than that for the other configurations, mainly because the variable-area exhaust nozzle in the wide-open position was too small to permit operation at as high fuel-air ratios as with the smaller-blocked-area configurations. This difference in the value of fuel-air ratio at which the variable-area exhaust nozzle is driven open is due to the variation in combustion efficiency for the different flame-holder configurations. Thus, the intersection of the lean blow-out limit with the maximum-area limit (fig. 11) occurs at lower altitudes as the blocked area is increased to 30.8 percent, because the combustion efficiency is increased. The maximum altitude limit obtained during this investigation was 59,700 feet, using flame holder 5 with a blocked area of 27.5 percent.

Effect of Trailing and Interconnecting Gutters

The effects on afterburner performance and operational limits of the addition of a trailing V-gutter and of interconnecting V-gutters to a 2-ring V-gutter flame holder are shown in figures 12 and 13. The configurations consist of a basic 2-ring V-gutter flame holder (1), the basic flame holder with interconnecting V-gutters (5), and the basic flame holder with a trailing V-gutter (10). The addition of interconnecting V-gutters increased the blockage of the original flame holder 5.2 percent, while the trailing V-gutter added 11.4-percent blocked area 5 inches downstream of the original flame holder. Therefore, the performance comparisons will include both the effect of interconnecting gutters and trailing gutters along with changes in percentage of blockage.

Both the connecting V-gutters and the trailing V-gutter increased the afterburner pressure loss in the same order as the blockage increased. The connecting gutters had very little effect on combustion efficiency and augmented net thrust ratio. The trailing V-gutter increased combustion efficiency about 8 points and thrust ratio 4 points at 1125 pounds per square foot, but had no effect on performance at 680 pounds per square foot.

The addition of connecting V-gutters to a basic V-gutter-type flame holder tended to improve the altitude limit of operation without decreasing the performance of the afterburner at the higher pressure levels investigated and also resulted in a considerable decrease in the fuel-air ratio at which lean blow-out occurred (fig. 13). This ability to support combustion at lower fuel-air ratios is probably due to seating of flame on the flame-holder ring, where conditions are more favorable to combustion, and then passing of the flame to the other ring by way of the connecting gutters. Therefore, a V-gutter flame holder with connecting V-gutters would give a wider range of fuel-flow operation right up to the maximum altitude operational limit.

The addition of a trailing V-gutter ring equally spaced radially between the two rings of the V-gutter flame holder had very little effect on the lean blow-out limit and decreased the altitude limit slightly at maximum exhaust-nozzle area because of higher combustion efficiency. The performance and operational characteristics of a flame holder with a trailing V-gutter are apparently similar to those of a flame holder with a comparable increase in blocked area. The data obtained in this investigation indicate no advantage in using a trailing V-gutter.

Effect of Altitude on V-Gutter Flame Holder

Flame holder 9 (2-ring V-gutter with connecting V-gutters having a blockage of 27 percent), which was shown to be among the more satisfactory of the V-gutter flame holders, was investigated over a range of afterburner-inlet pressure from 3130 to 680 pounds per square foot, which corresponds to an altitude range from 15,000 to 50,000 feet at a flight Mach number of 0.60. In addition to afterburner total-pressure loss, combustion efficiency, and augmented net thrust ratio, parameters of exhaust-gas total temperature and specific fuel consumption based on net thrust are presented for the range of operable afterburner fuel-air ratio (fig. 14).

Afterburner total-pressure loss indicates no definite trend as afterburner-inlet total pressure is decreased; the maximum total-pressure loss for the entire afterburner is approximately 0.14 at a fuel-air ratio of 0.05. For a given afterburner-inlet total pressure, as the fuel-air ratio is increased, the combustion efficiency remains fairly constant up to a fuel-air ratio of 0.04 and then begins to decrease while the exhaust-gas temperature, the augmented net thrust ratio, and the specific fuel consumption increase over the entire range of fuel-air ratio. For a given fuel-air ratio, as the afterburner-inlet total pressure is reduced, the combustion efficiency decreases, with a resulting decrease in exhaust-gas temperature and augmented net thrust ratio and a corresponding increase in specific fuel consumption. Varying the afterburner-inlet total pressure from 3130 to 680 pounds per square foot decreased the peak

combustion efficiency from 0.92 to 0.57, the maximum exhaust-gas temperature from 3100° to 2800° R, and the maximum net thrust augmentation ratio (for wide-open exhaust nozzle) from 1.46 to 1.32; while the specific fuel consumption for maximum thrust increased from 2.35 to 3.0.

CONCLUDING REMARKS

An investigation of ten flame holders in a full-scale louvered-liner afterburner (no combustion screech encountered over the range of afterburner inlet total pressures from 3130 to 680 lb/sq ft) was conducted to determine the effects of flame-holder design on performance. A uniform fuel-air ratio distribution for a typical velocity profile at the flame-holder inlet was established in order that the effects of the relations among diffuser, fuel-system, and flame-holder designs might be eliminated from the results. However, because data obtained from any investigation are limited by the particular environment, the results presented herein are applicable to typical afterburners with louvered cooling liners.

A V-gutter flame holder had consistently higher combustion efficiency and altitude operating limits than a U-gutter flame holder. The difference in combustion efficiency could not be completely eliminated by adding louvers to the U-gutter, but this addition did overcome the difference in altitude limits. The addition of a downstream surface to the V-gutter had a favorable effect on combustion efficiency at high afterburner pressures because of the presence of the hot metal surface in the gutter wake, but had negligible effect on performance at low pressures.

The data showed no marked superiority of either a 2- or a $1\frac{1}{2}$ -inch-wide gutter over the other. However, decreasing the gutter width to $1\frac{1}{2}$ inch resulted in severe decreases in afterburner performance and operational limits. Selection of a proper gutter width must be accompanied by proper radial positioning of the gutters with respect to the velocity profile, in order to ensure satisfactory performance.

Increasing the flame-holder blocked area from 22.3 to 30.8 percent increased the afterburner combustion efficiency approximately 15 and 8 points at afterburner-inlet total pressures of 1125 and 680 pounds per square foot, respectively. Using interconnecting gutters between the rings of a flame holder aided propagation of the flame from one ring to another, shifted the lean blow-out to lower fuel-air ratios, and thus improved the altitude operational characteristics of the afterburner without loss in performance at the higher pressure levels investigated.

Lewis Flight Propulsion Laboratory
National Advisory Committee for Aeronautics
Cleveland, Ohio, August 21, 1953

APPENDIX - CALCULATIONS

Symbols

The following symbols are used in the calculations and the figures:

A	cross-sectional area, sq ft
C_V	velocity coefficient
F_j	jet thrust, lb
F_n	net thrust, lb
f	fuel-air ratio
g	acceleration due to gravity, 32.2 ft/sec ²
h	enthalpy, Btu/lb
h_c	lower heating value of fuel, Btu/lb
P	total pressure, lb/sq ft abs
p	static pressure, lb/sq ft abs
R	gas constant, 53.4 ft-lb/(lb)(°R)
T	total temperature, °R
V	velocity, ft/sec
W_a	air flow, lb/sec
W_f	fuel flow, lb/hr
W_f/F_n	specific fuel consumption, lb/(hr)(lb thrust)
W_g	gas flow, lb/sec
γ	ratio of specific heats for gases
η	combustion efficiency

Subscripts:

a air
b afterburner
e engine
m fuel manifold
s labyrinth seal
T total
cl compressor leakage
tc turbine cooling
nc nozzle cooling
tp turbine pump

Stations:

0 free-stream conditions
1 engine inlet
2 compressor inlet
3 compressor outlet
5 turbine outlet
9 exhaust-nozzle inlet
n exhaust-nozzle outlet

Methods of Calculations

Air flow. - Engine-inlet air flow was determined from pressure and temperature measurements obtained at the engine inlet by the following equation:

$$W_{a,1} = A_1 P_1 \sqrt{\frac{g}{RT_1}} \sqrt{\frac{2\gamma_1}{\gamma_1 - 1} \left(\frac{P_1}{P_1}\right)^{\frac{\gamma_1 - 1}{\gamma_1}} \left[\left(\frac{P_1}{P_1}\right)^{\frac{\gamma_1 - 1}{\gamma_1}} - 1 \right]}$$

From previous investigations, it was found that air was leaking from sheet-metal joints between stations 1 and 2, from open bolt holes at the compressor inlet, and from twelfth-stage de-icing air lines. After an attempt was made to plug these leaks, a correlation between gas flow at the exhaust-nozzle outlet and inlet air flow was obtained. With the assumption that all unmeasured leakage occurred between stations 1 and 2, the following relation was obtained:

$$W_{a,2} = 0.98 W_{a,1}$$

Air flow at the compressor outlet (station 3) was obtained by subtracting from the air flow at station 2 the compressor leakage, the turbine- and nozzle-cooling air flows, and the compressor bleed air used to drive the air turbine fuel pump:

$$W_{a,3} = W_{a,2} - W_{a,cl} - W_{a,tc} - W_{a,nc} - W_{a,tp}$$

Gas flow. - The engine gas flow at the turbine outlet is

$$W_{g,5} = W_{a,3} + \frac{W_{f,e}}{3600} + W_{a,tc}$$

and the afterburner gas flow is

$$W_{g,b} = W_{a,3} + \frac{W_{f,e} + W_{f,b}}{3600} + W_{a,tc}$$

Fuel-air ratio. - The engine fuel-air ratio is given by the following equation:

$$f_e = \frac{W_{f,e}}{3600 W_{a,3}}$$

The afterburner fuel-air ratio used herein is defined as the weight flow of fuel injected into the afterburner plus the unburned engine fuel divided by the weight flow of unburned air entering the afterburner.

When air flow, engine fuel flow, afterburner fuel flow, and engine combustion efficiency are combined, the following equation for afterburner fuel-air ratio is obtained:

$$f_b = \frac{(1 - \eta_e)W_{f,e} + W_{f,b}}{3600(W_{a,3} + W_{a,tc}) - \frac{\eta_e W_{f,e}}{0.0675}}$$

where 0.0675 is the stoichiometric fuel-air ratio for the engine fuel. The total fuel-air ratio for the engine and afterburner is

$$f_T = \frac{W_{f,e} + W_{f,b}}{3600(W_{a,3} + W_{a,tc})}$$

Augmented thrust. - The jet thrust of the combined engine and afterburner configuration was determined from the thrust system measurements by the equation

$$F_j = F_d + (A_s - A_9)(P_1 - p_s) + A_9(P_1 - p_0) + 0.80\left(\frac{1}{2} \frac{W_{a,1}}{g} V_0\right)$$

where F_d is the thrust system scale reading adjusted for the pressure difference on the link connecting the thrust bed in the test chamber and the thrust-measuring cell outside the test chamber. The term $0.80\left(\frac{1}{2} \frac{W_{a,1}}{g} V_0\right)$ is the momentum force existing at the bellmouth.

The augmented net thrust was obtained by subtracting the free-stream momentum of the inlet air from the jet thrust:

$$F_n = F_j - \frac{W_{a,1}}{g} V_0$$

Standard engine thrust. - The jet thrust obtainable with the standard engine at rated speed was calculated from measurements of turbine-outlet total pressure and temperature and gas flow obtained during the afterburning program:

$$F_{j,e} = C_V \left[\frac{W_{g,5}}{g} V_n + A_n (p_n - p_0) \right]$$

where V_n and p_n are conditions existing at the exhaust nozzle exit and were determined by applying the standard engine tail-pipe total-pressure loss to P_5 , $P_9' = 0.096 P_5$. The nozzle velocity coefficient was assumed to be 0.99.

The standard engine net thrust was obtained by subtracting the free-stream momentum of the inlet air from the jet thrust:

$$F_{n,e} = F_{j,e} - \frac{W_{a,1}}{g} V_0$$

Exhaust-gas total temperature. - The exhaust-gas total temperature was calculated from the jet thrust and conditions existing at the exhaust nozzle:

$$T_n = \frac{g F_j^2}{c_{Vg}^2 W_{g,9}^2 \left(\frac{2R\gamma_9}{\gamma_9 - 1} \right) \left[1 - \left(\frac{P_0}{P_9} \right)^{\frac{\gamma_9 - 1}{\gamma_9}} \right]}$$

Engine combustion efficiency. - Engine combustion efficiency is the ratio of enthalpy rise through the engine divided by the product of engine fuel flow and the lower heating value of the fuel:

$$\eta_e = \frac{h_a \left[\frac{T_5}{T_1} + f_e \lambda \right] \frac{T_5}{T_m}}{f_e h_c}$$

where λ is equivalent to the term $(Am + B)/(m + 1)$ which accounts for the difference between the enthalpy of carbon dioxide and water vapor in the burned mixture and the enthalpy of oxygen removed from the air by their formation (symbols of ref. 5).

Afterburner combustion efficiency. - Afterburner combustion efficiency was obtained by dividing the enthalpy rise through the afterburner by the product of afterburner fuel flow and lower heating value of the fuel:

$$\eta_b = \frac{h_a \left[\frac{T_n}{T_1} + f_T \lambda \right] \frac{T_n}{T_m} - \eta_e f_e h_c}{h_c f_T - \eta_e f_e h_c}$$

Specific fuel consumption. - The specific fuel consumption based on net thrust is given by the following equation:

$$\frac{W_f}{F_n} = \frac{W_{f,e} + W_{f,b}}{F_n}$$

REFERENCES

1. Conrad, E. William, and Jansen, Emmert T.: Effects of Internal Configuration on Afterburner Shell Temperatures. NACA RM E51I07, 1952.
2. Grey, Ralph E., Krull, H. G., and Sargent, A. F.: Altitude Investigation of 16 Flame-Holder and Fuel-System Configurations in Tail-Pipe Burner. NACA RM E51E03, 1951.
3. Conrad, E. William, and Campbell, Carl E.: Altitude Investigation of Several Afterburner Configurations for the J40-WE-8 Turbojet Engine. NACA RM E52L10, 1953.
4. Fleming, W. A., Conrad, E. William, and Young, A. W.: Experimental Investigation of Tail-Pipe-Burner Design Variables. NACA RM E50K22, 1951.
5. Turner, L. Richard, and Bogart, Donald: Constant-Pressure Combustion Charts Including Effects of Diluent Addition. NACA Rep. 937, 1949. (Supersedes NACA TN's 1086 and 1655.)

3002

TABLE I. - FLAME HOLDERS INVESTIGATED

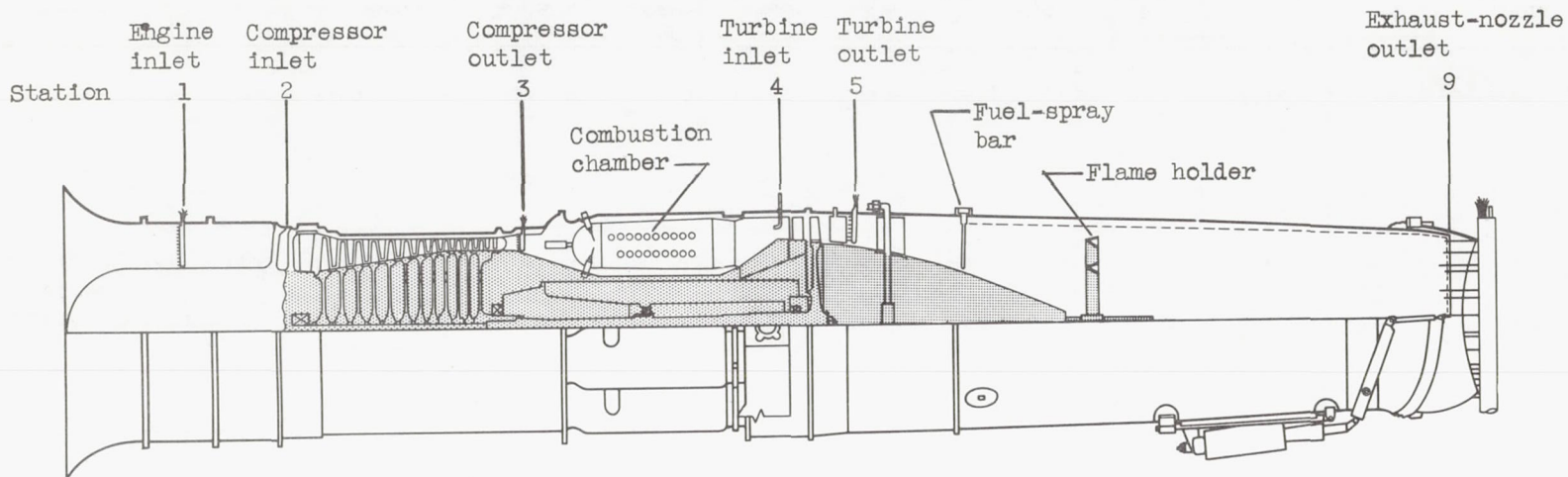


Flame holder		1	2	3	4	5	6	7	8	9	10
General description of flame holder		2-ring V	2-ring closed V	2-ring U	2-ring U, louvered	2-ring V	2-ring V	3-ring V	9-ring V	2-ring V	2-ring V with trailing V
Blockage of flame holder, percent		22.3	22.4	22.2	22.2	27.5	30.8	30.9	28.1	27.1	33.7
Width of gutter, in.	Outer	2.00	2.00	2.00	2.00	2.00	2.00	1.50	All	1.56	2.00
	Inner	2.00	2.00	2.00	2.00	2.00	1.98	1.50 1.20	0.50	1.69	2.00 2.00
Diameter of flame-holder rings, in.		22.50 7.50	22.50 7.50	21.50 7.00	21.50 7.00	22.50 7.50	25.25 13.04	25.13 16.88 8.63	27.60 24.70 21.80 18.90 16.20 13.20 10.20 7.30 4.40	25.13 16.88	22.50 7.50 and trailing V, 15.00
Connecting gutters	Number	None	None	None	None	4	None	6	None	4	None
	Width, in.					2.00		1.40		1.63	

CONFIDENTIAL

NACA RM E53H15

CONFIDENTIAL



Station	Total-pressure probes	Wall and rake static-pressure probes	Thermocouples
1	24	10	12
3	12	2	12
4	8	--	8
5	15	3	24
9	13	4	--

NACA
CD-3039

Figure 1. - Schematic sketch of turbojet engine and afterburner showing instrumentation stations.

CONFIDENTIAL

CONFIDENTIAL

NACA RM E53H15

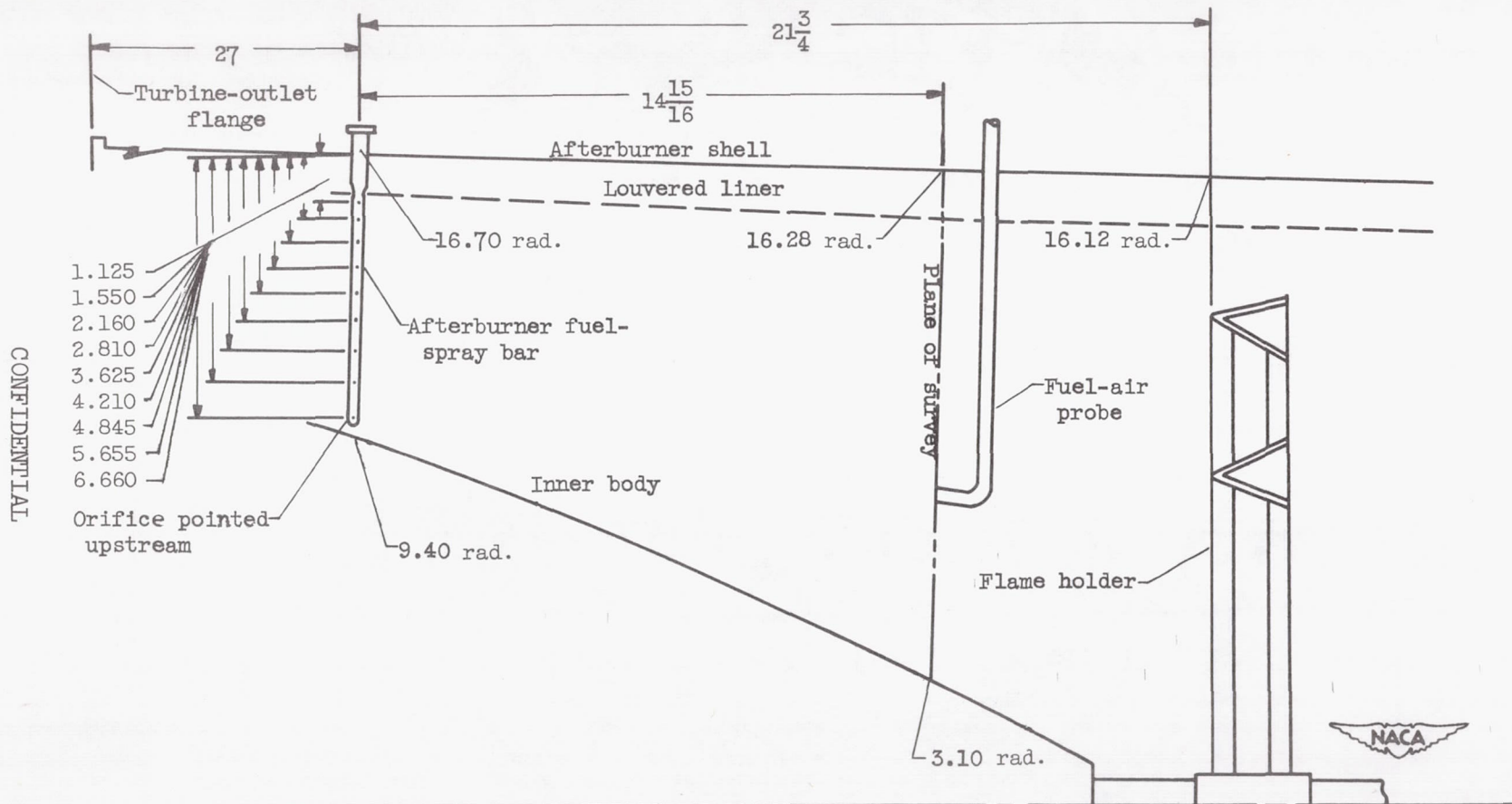


Figure 2. - Sketch of afterburner section showing details of fuel-spray bars, fuel-air survey station, and flame-holder location. (Dimensions are in inches.)

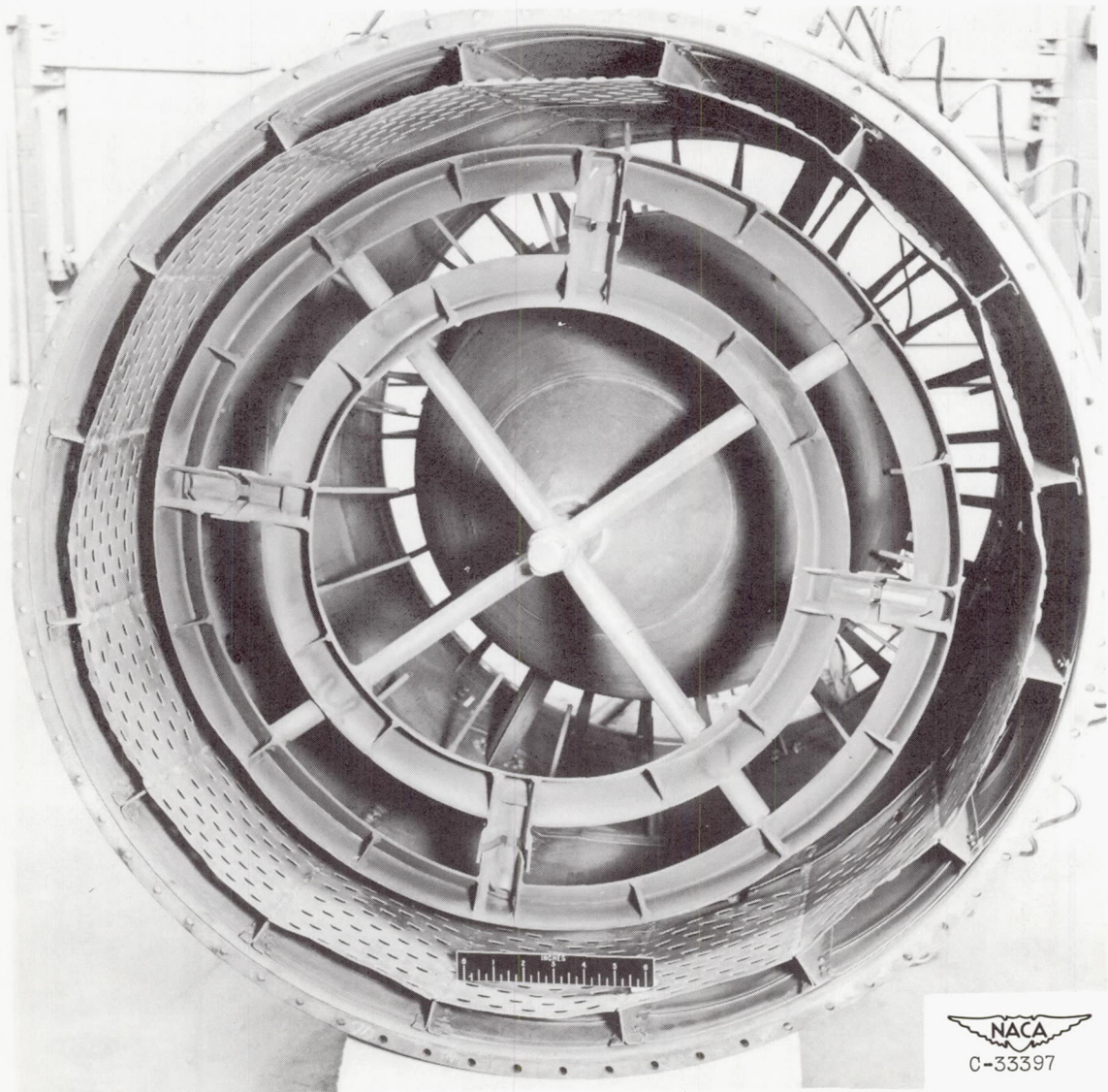


Figure 3. - Flame holder 9 mounted in afterburner.

3002

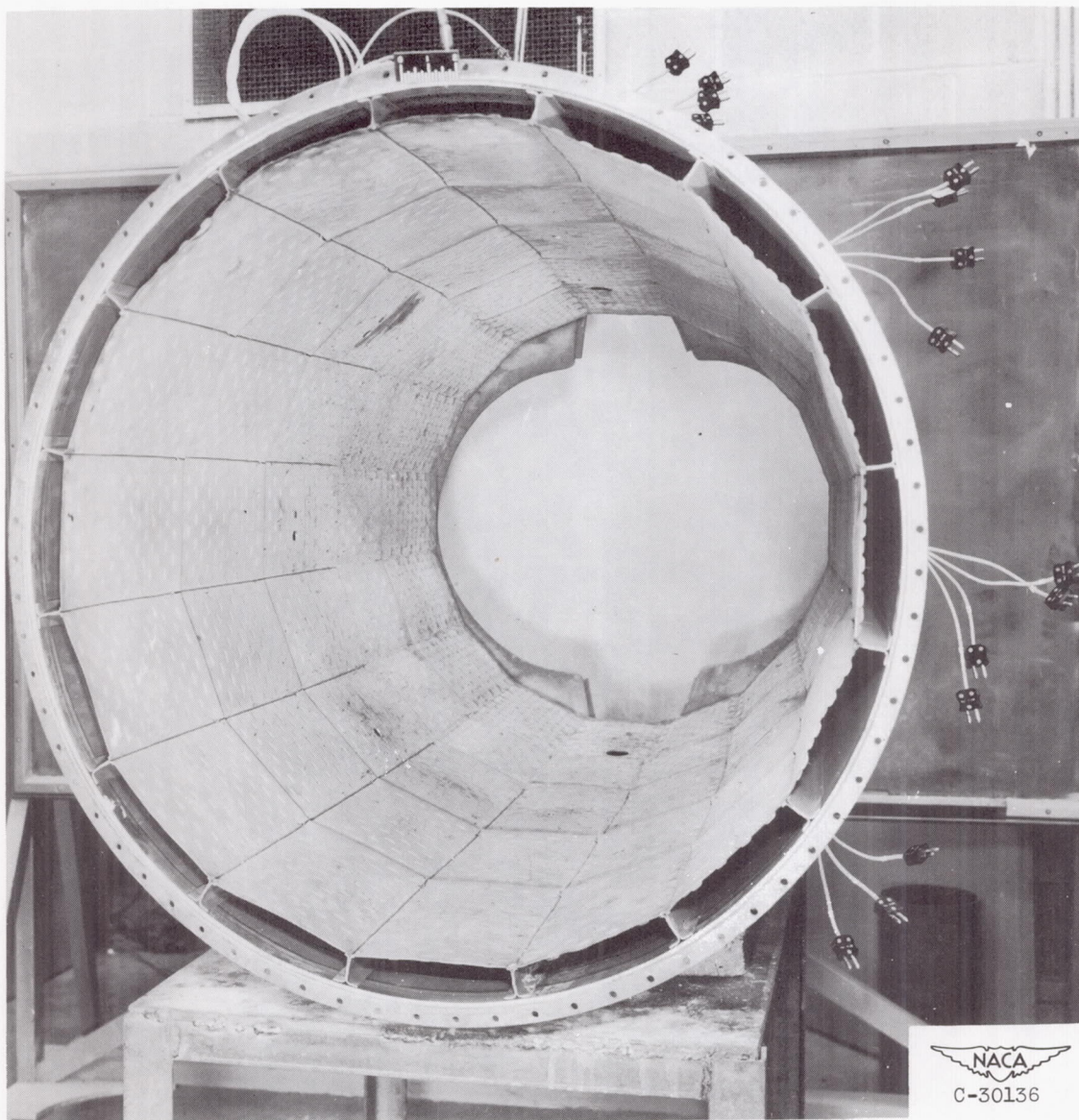
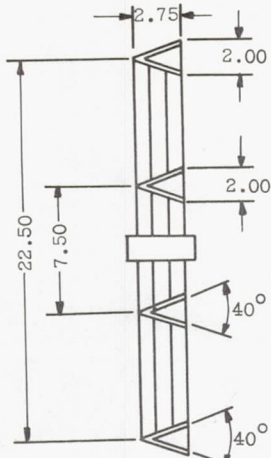
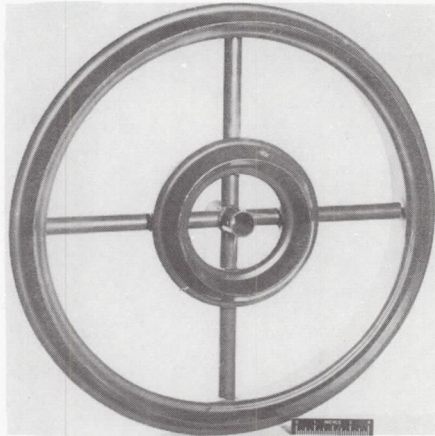
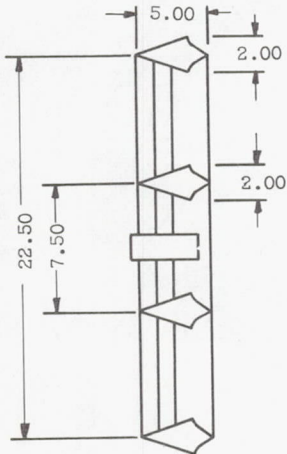


Figure 4. - Louvered afterburner liner.

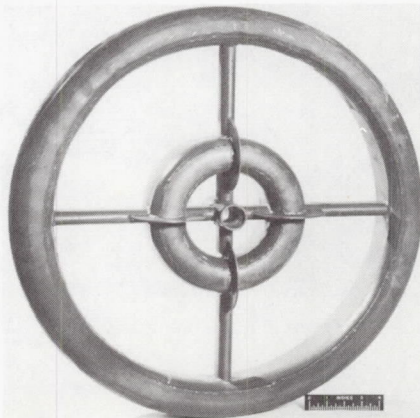
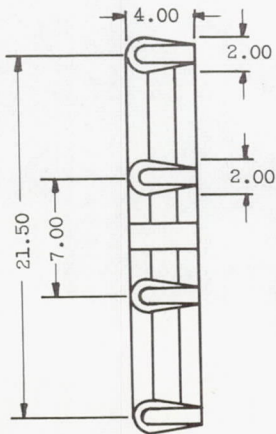


(a) Flame holder 1.: (Photograph not available.)



NACA
C-33398

(b) Flame holder 2.

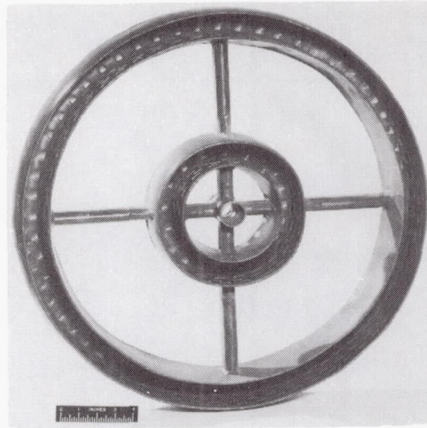
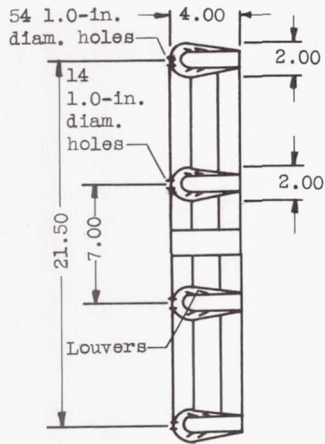


NACA
C-33399

(c) Flame holder 3.

Figure 5. - Cross sections and photographs of flame holders investigated. (Dimensions are in inches.)

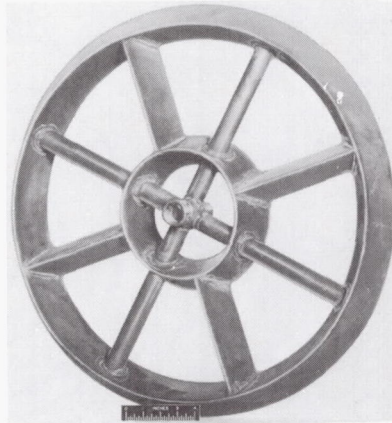
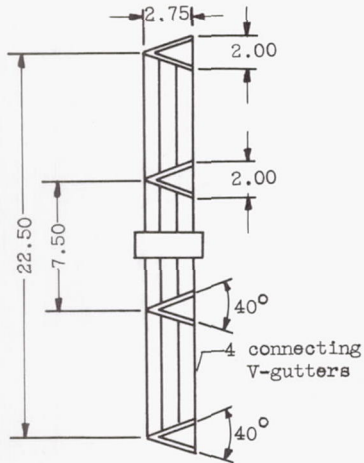
3002



NACA
C-33400

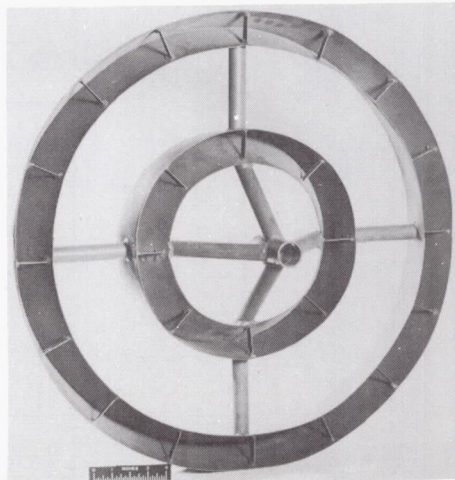
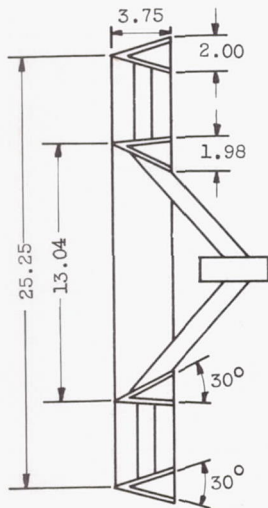
(d) Flame holder 4.

CS-4



NACA
C-33401

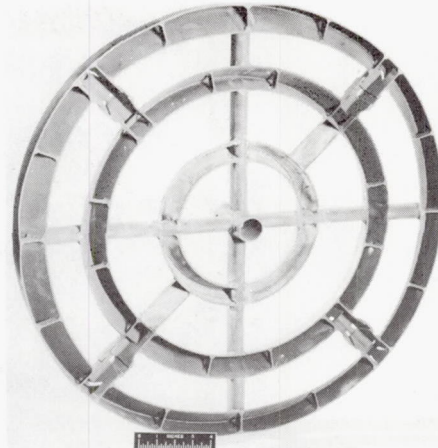
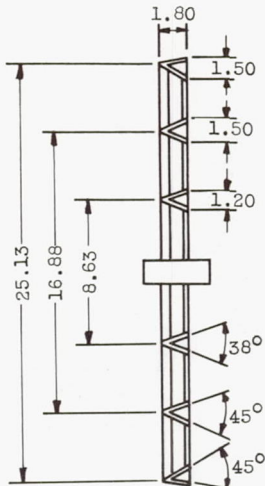
(e) Flame holder 5.



NACA
C-33402

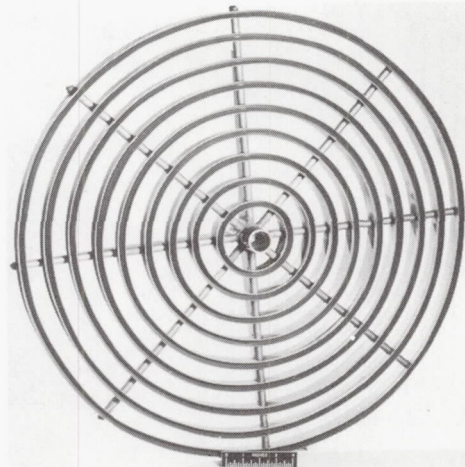
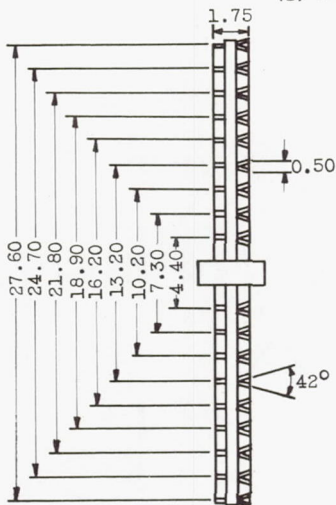
(f) Flame holder 6.

Figure 5. - Continued. Cross sections and photographs of flame holders investigated. (Dimensions are in inches.)



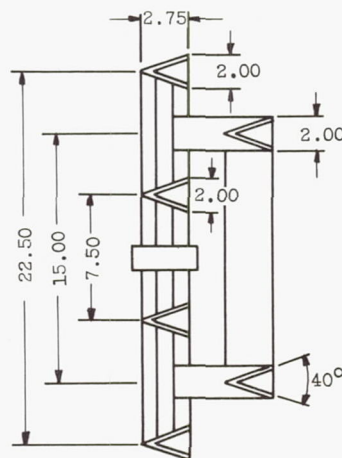
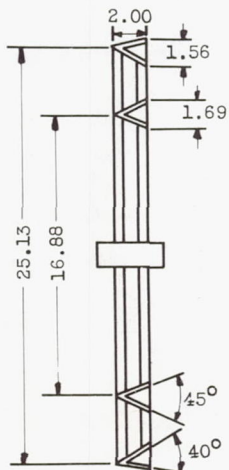
NACA
C-33403

(g) Flame holder 7.



NACA
C-33404

(h) Flame holder 8.



(i) Flame holder 9.

(j) Flame holder 10.

(Photo shown in figure 3.)

(Photo not available.)

Figure 5. - Concluded. Cross sections and photographs of flame holders investigated. (Dimensions are in inches.)

CS-4 back 3002

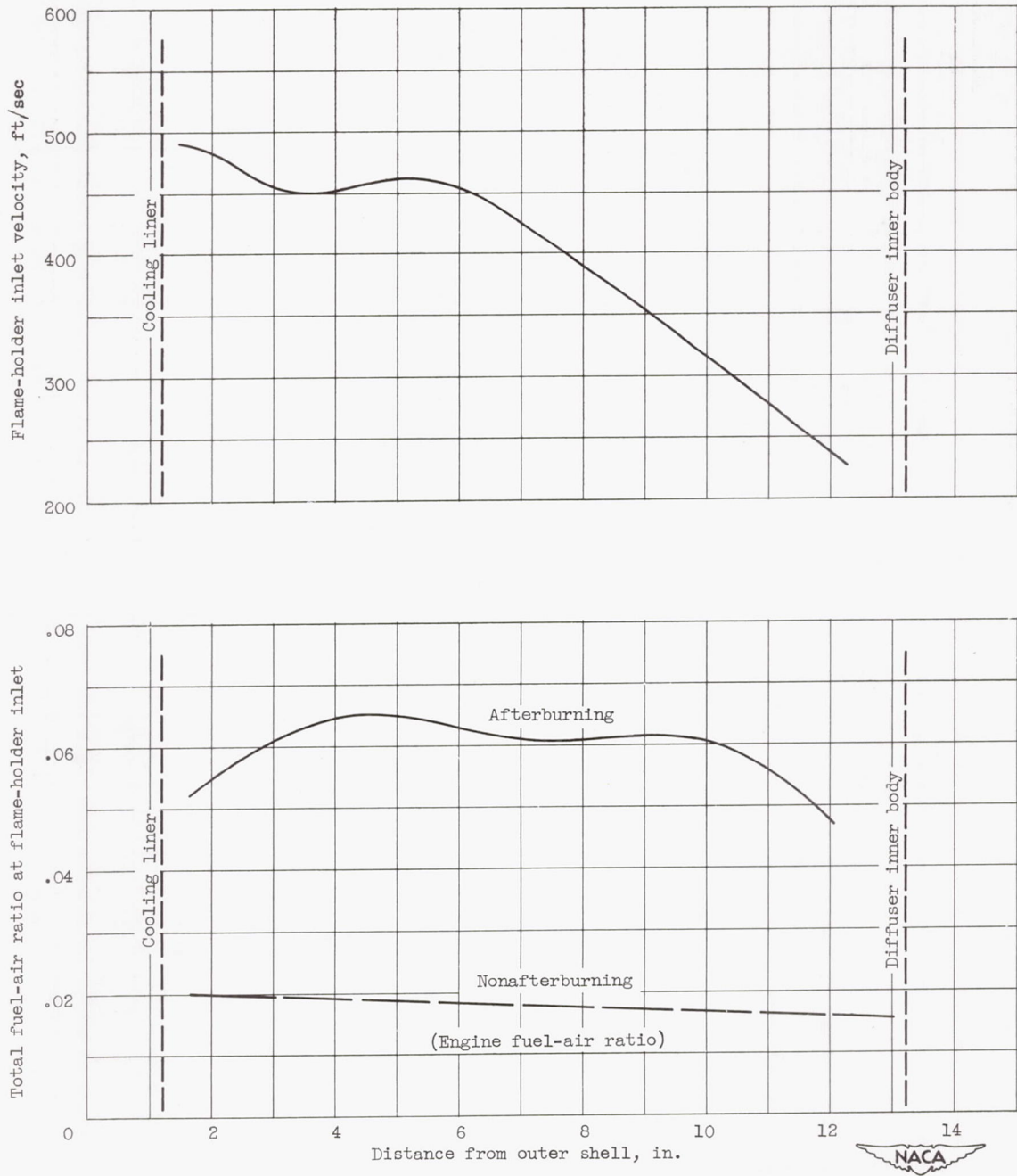
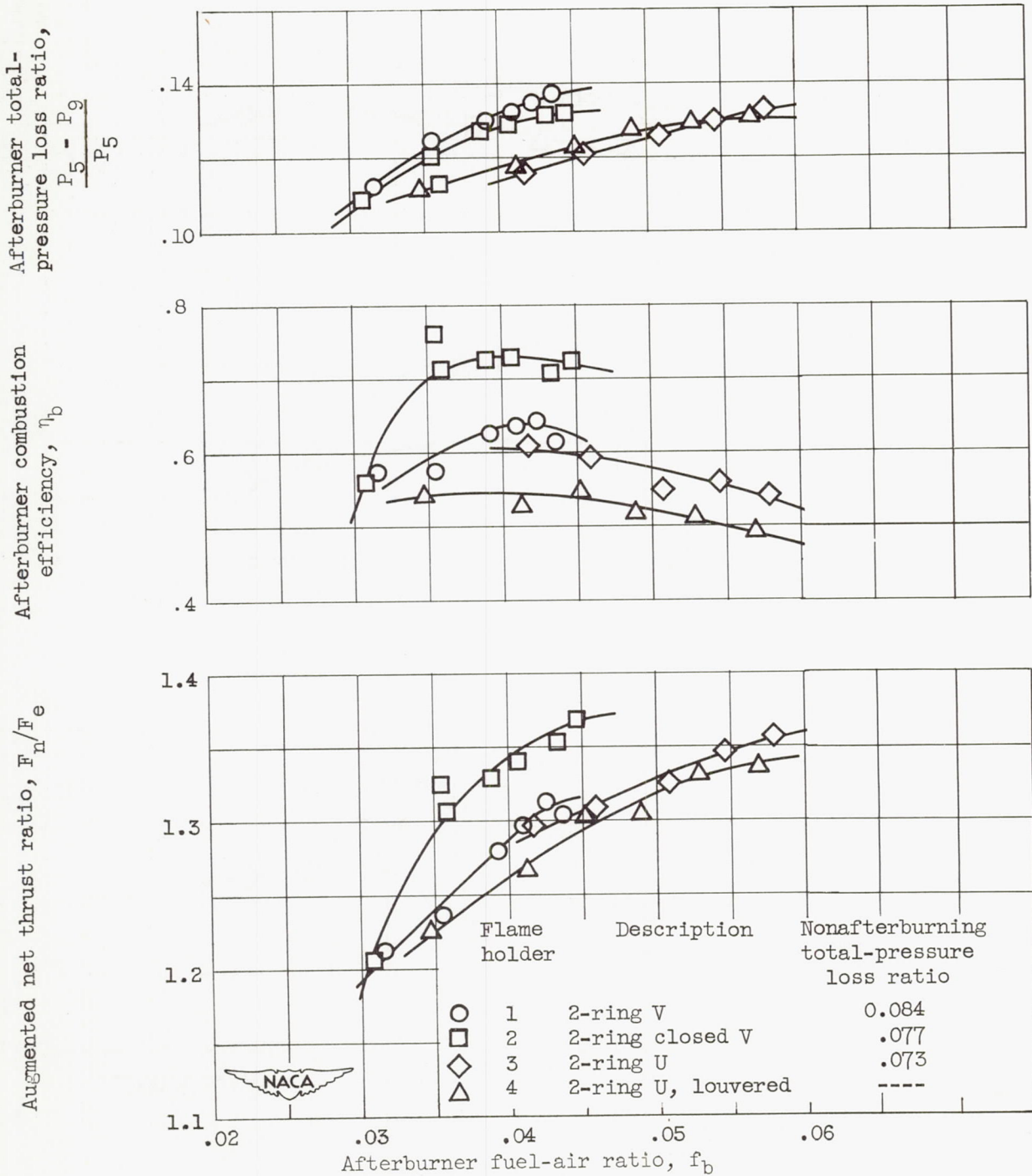


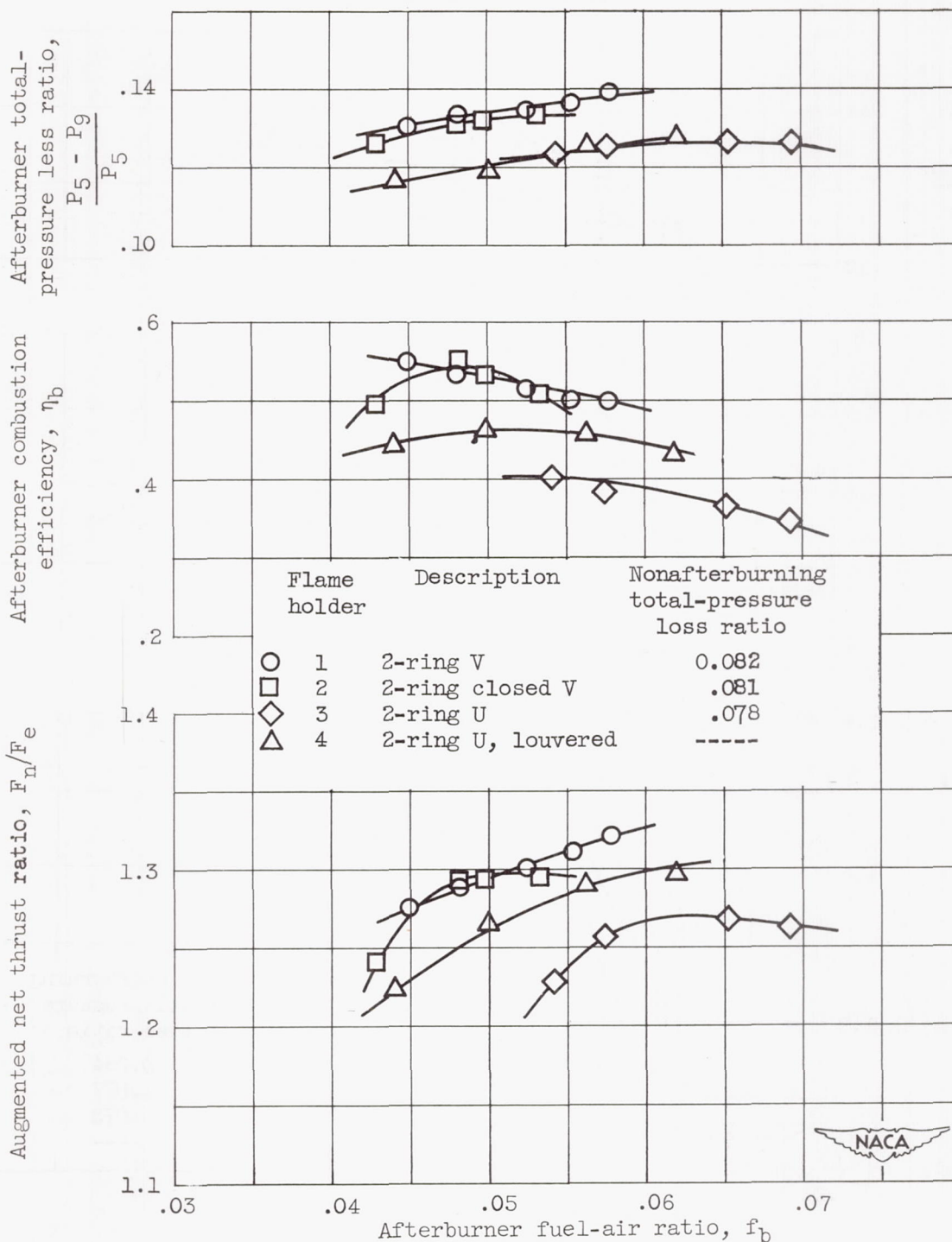
Figure 6. - Typical velocity and total fuel-air-ratio profiles at flame-holder inlet. Afterburner-inlet total pressure, 1125 pounds per square foot.



(a) Afterburner-inlet total pressure, 1125 pounds per square foot.

Figure 7. - Effect of shape of flame-holder gutter cross section on afterburner performance. Afterburner-inlet temperature, 1810° R.

3002



(b) Afterburner-inlet total pressure, 680 pounds per square foot.

Figure 7. - Concluded. Effect of shape of flame-holder gutter cross section on afterburner performance. Afterburner-inlet temperature, 1810° R.

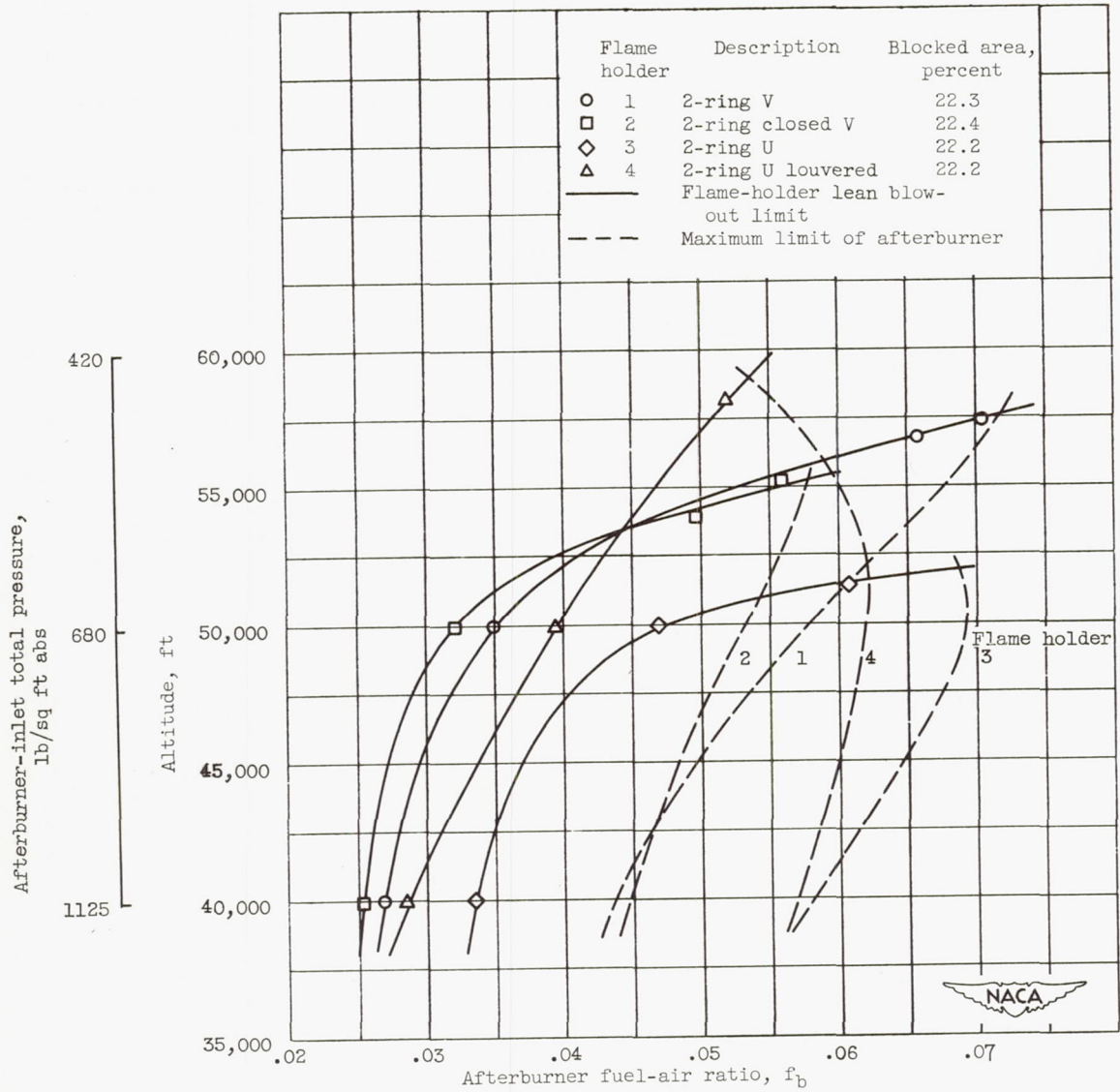


Figure 8. - Effect of shape of flame-holder gutter cross section on afterburner operational limits. Flight Mach number, 0.60.

3002

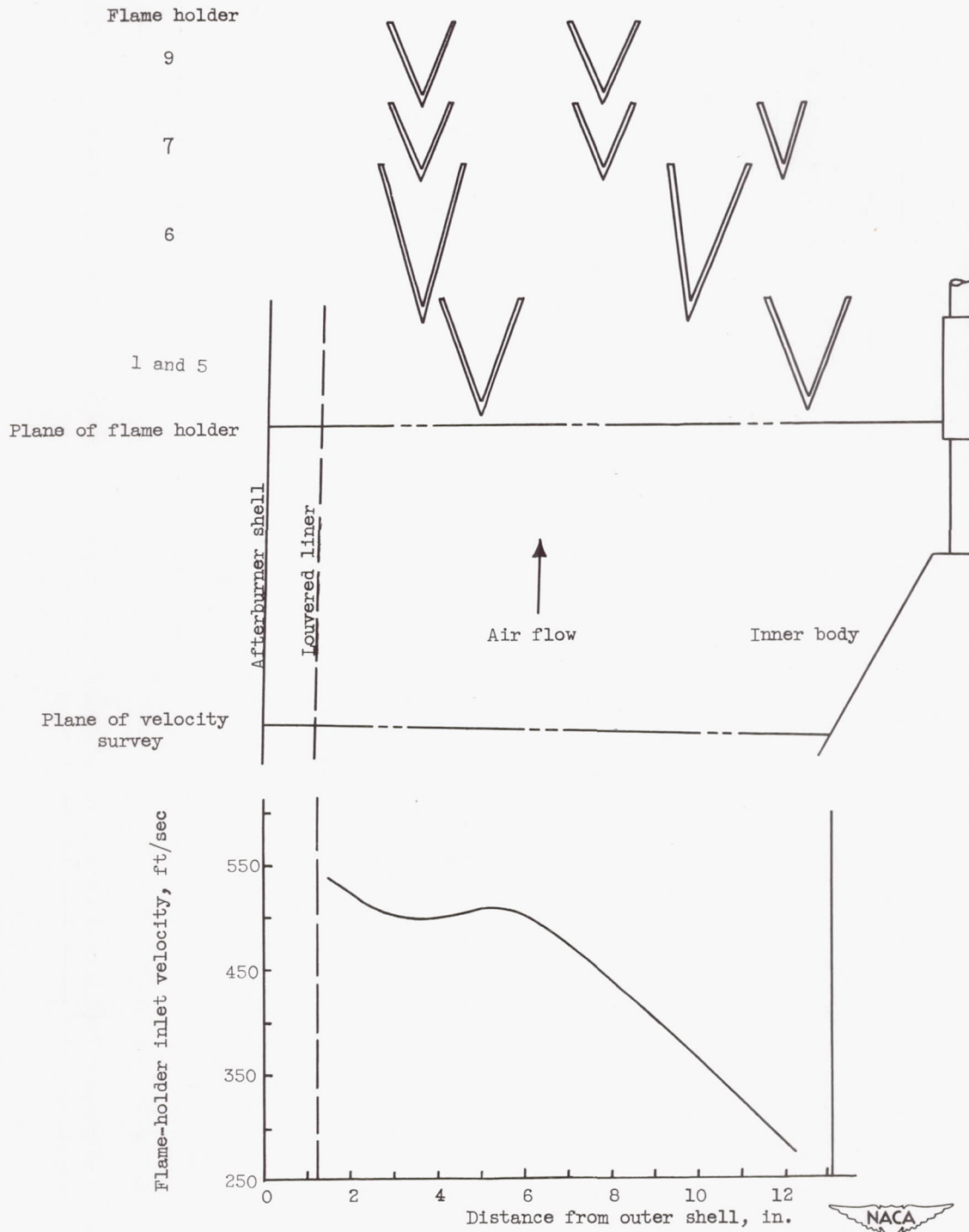
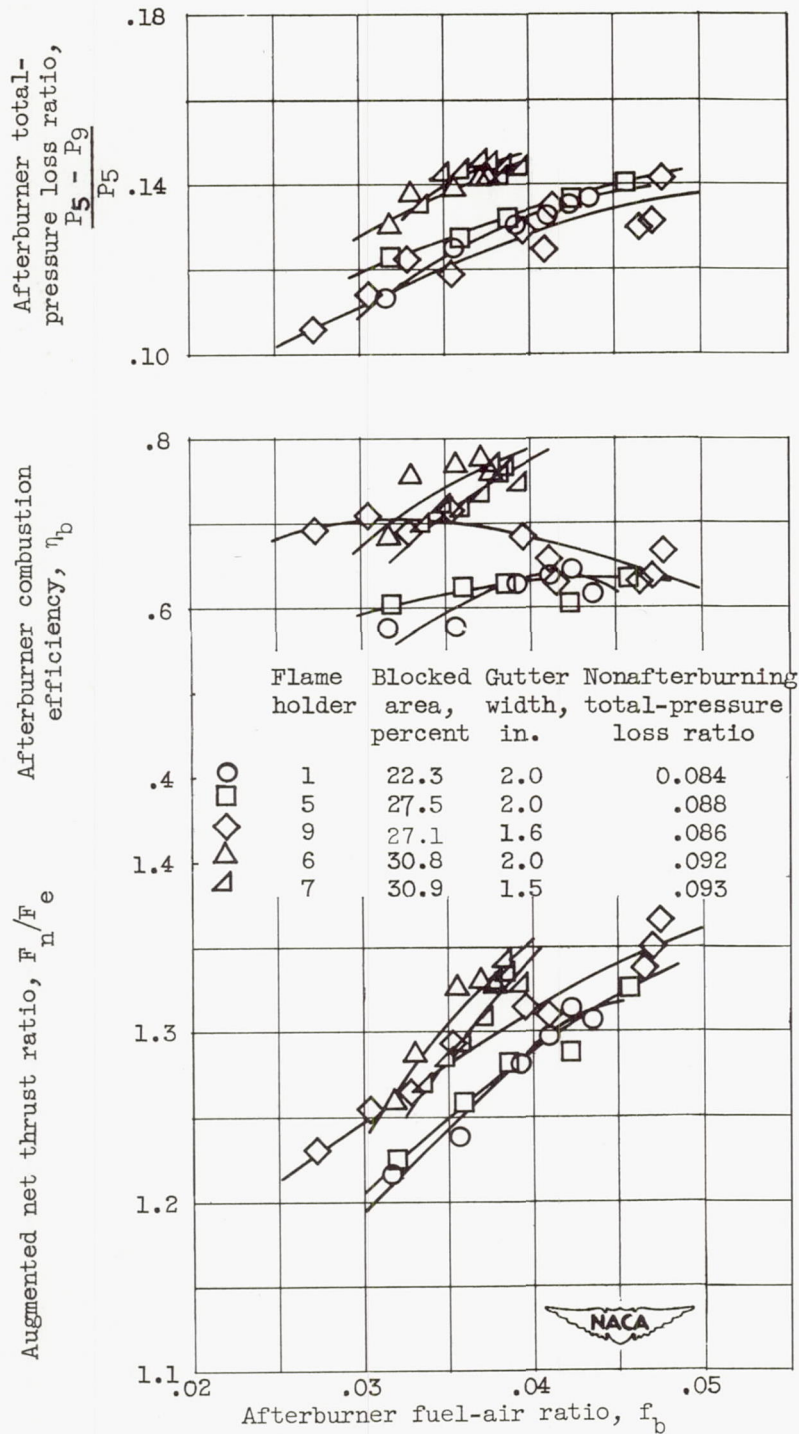


Figure 9. - Location of V-gutters of flame holders 1, 5, 6, 7, and 9 with reference to typical flame-holder inlet velocity. Afterburner-inlet total pressure, 1125 pounds per square foot.

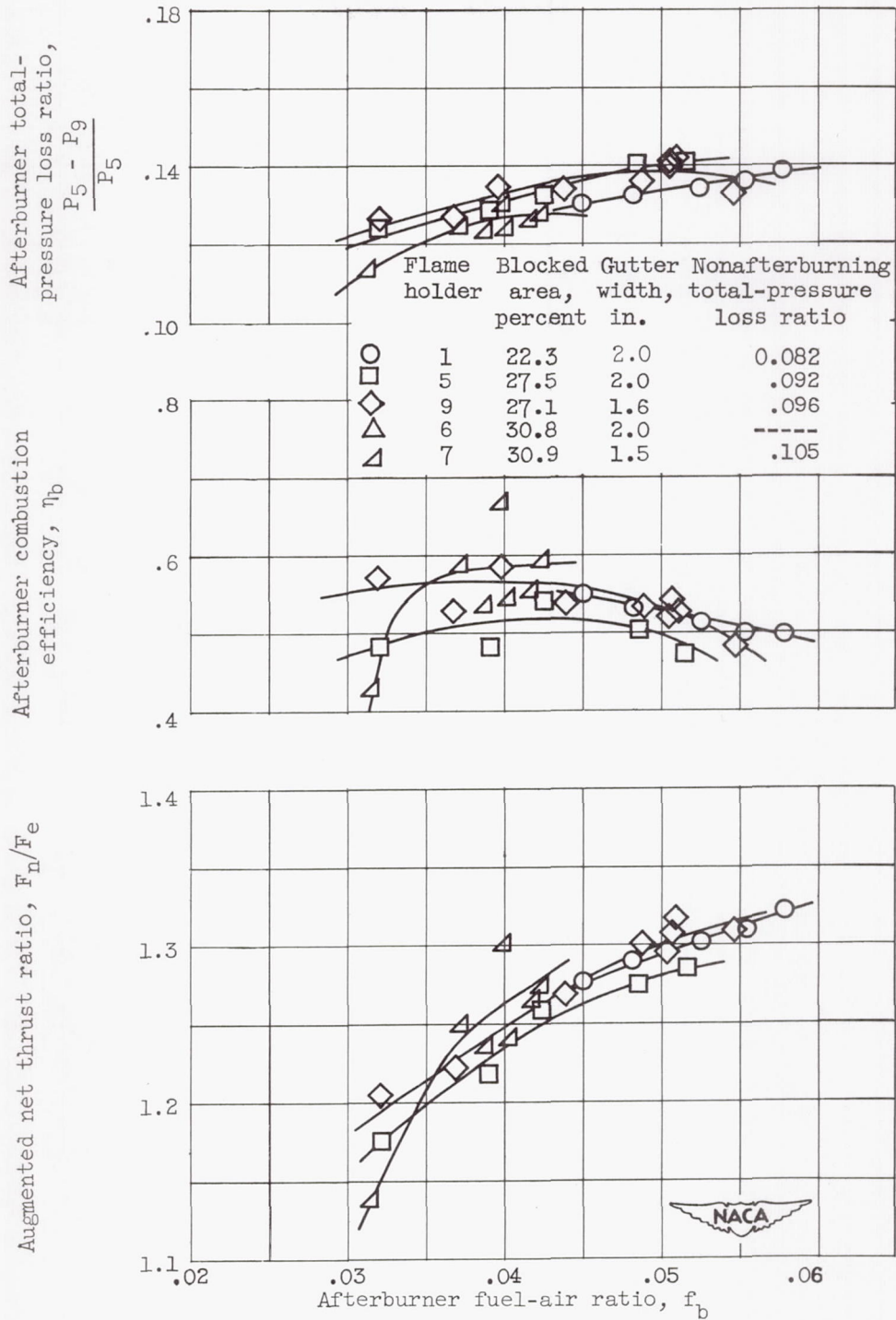


(a) Afterburner-inlet total pressure, 1125 pounds per square foot.

Figure 10. - Effect of gutter width and blocked area of V-gutter flame holders on afterburner performance. Afterburner-inlet temperature, 1810° R.

3002

CS-5



(b) Afterburner-inlet total pressure, 680 pounds per square foot absolute.

Figure 10. - Concluded. Effect of gutter width and blocked area of V-gutter flame holders on afterburner performance. Afterburner-inlet temperature, 1810° R.

3002

CS-5 back

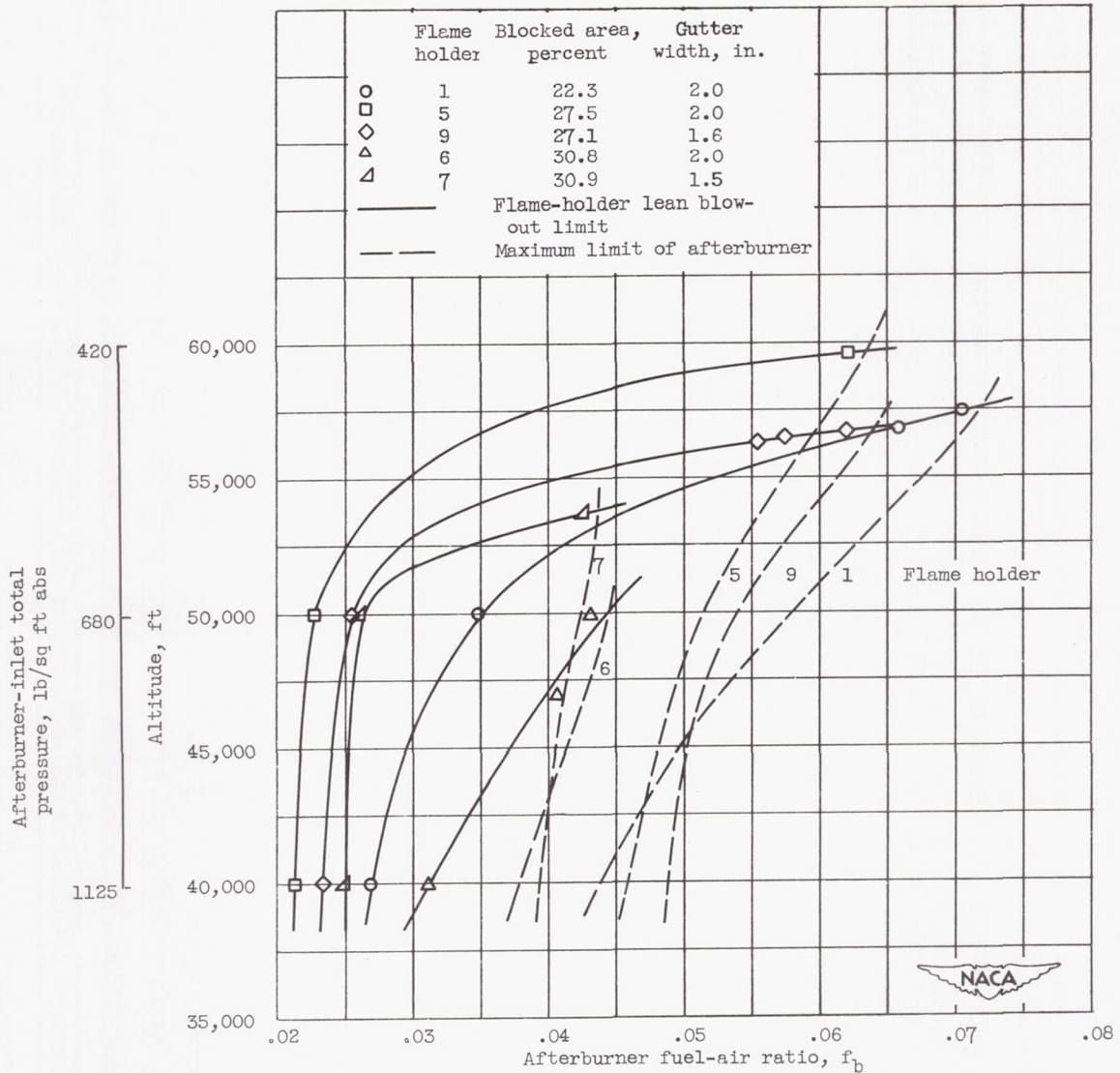
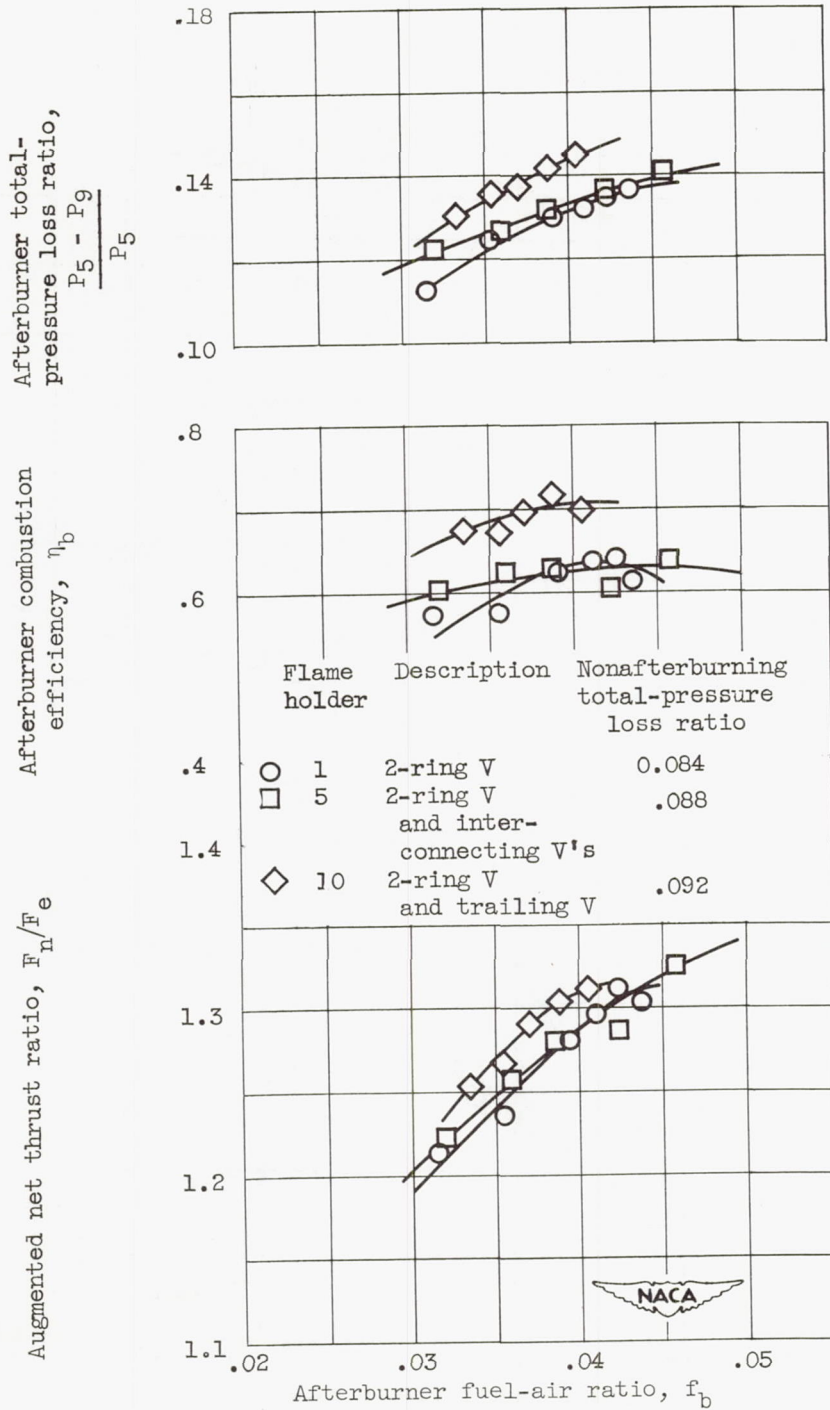
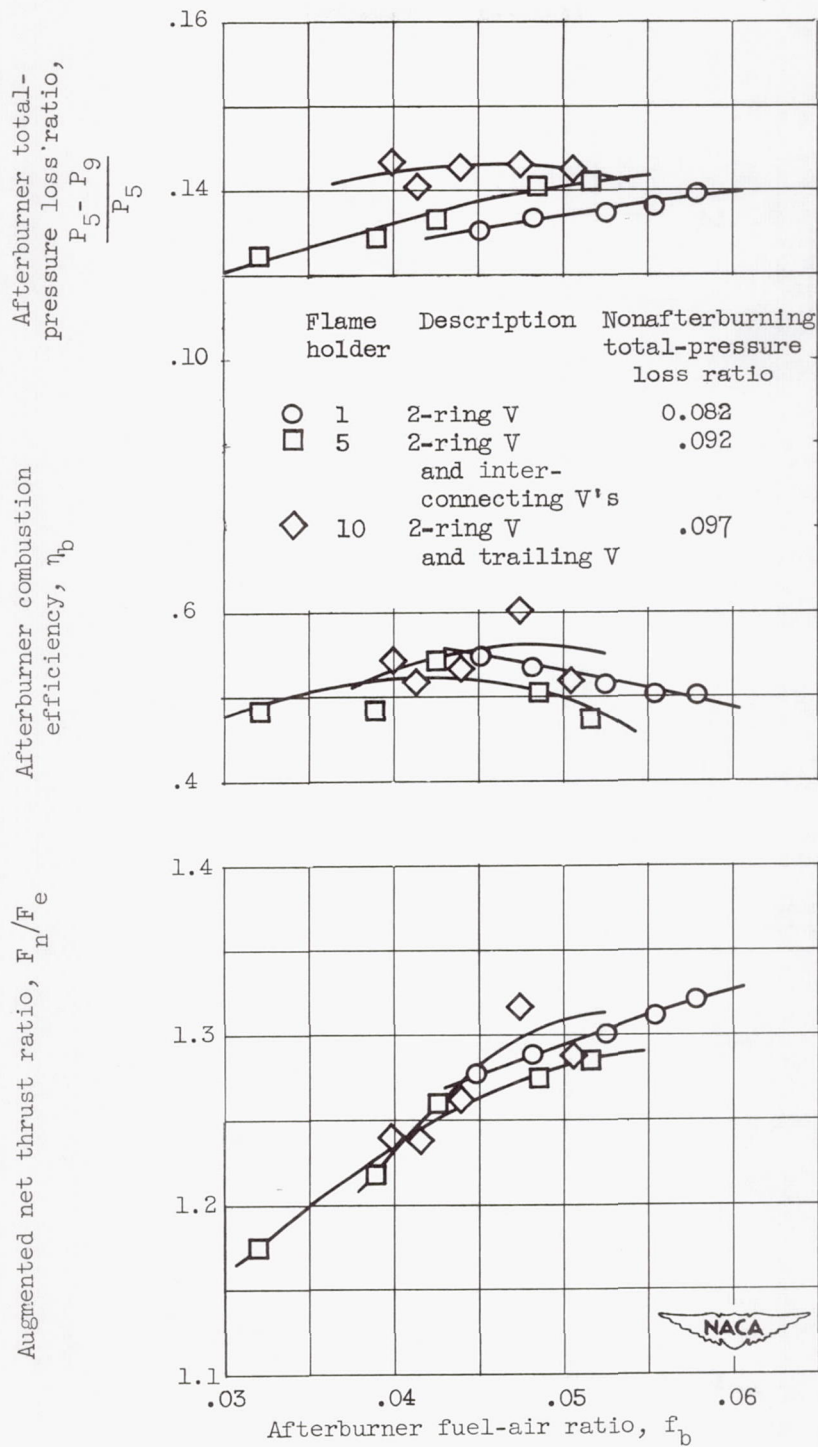


Figure 11. - Effect of gutter width and blocked area of V-gutter flame holders on afterburner operational limits. Flight Mach number, 0.60.



(a) Afterburner-inlet total pressure, 1125 pounds per square foot.

Figure 12. - Effect of addition of trailing V-gutter and interconnecting V-gutters to 2-ring V-gutter flame holder on afterburner performance. Afterburner-inlet temperature, 1810° R.



(b) Afterburner-inlet total pressure 680 pounds per square foot.

Figure 12. - Concluded. Effect of addition of trailing V-gutter and interconnecting V-gutters to 2-ring V-gutter flame holder on afterburner performance. Afterburner-inlet temperature, 1810° R.

3002

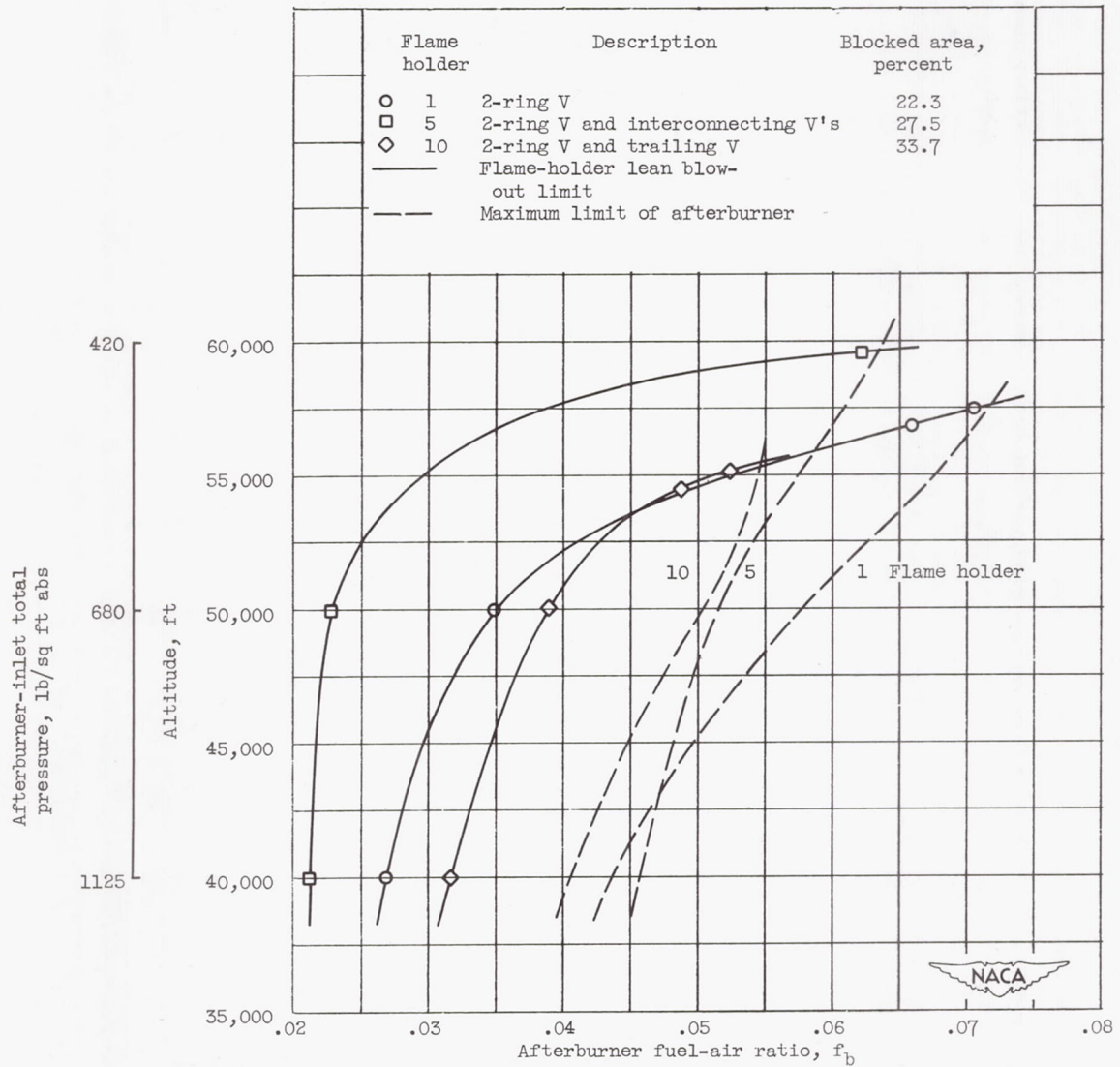


Figure 13. - Effect of addition of trailing V-gutter and interconnecting V-gutter to 2-ring V-gutter flame holder on afterburner operational limits. Flight Mach number, 0.60.

3002

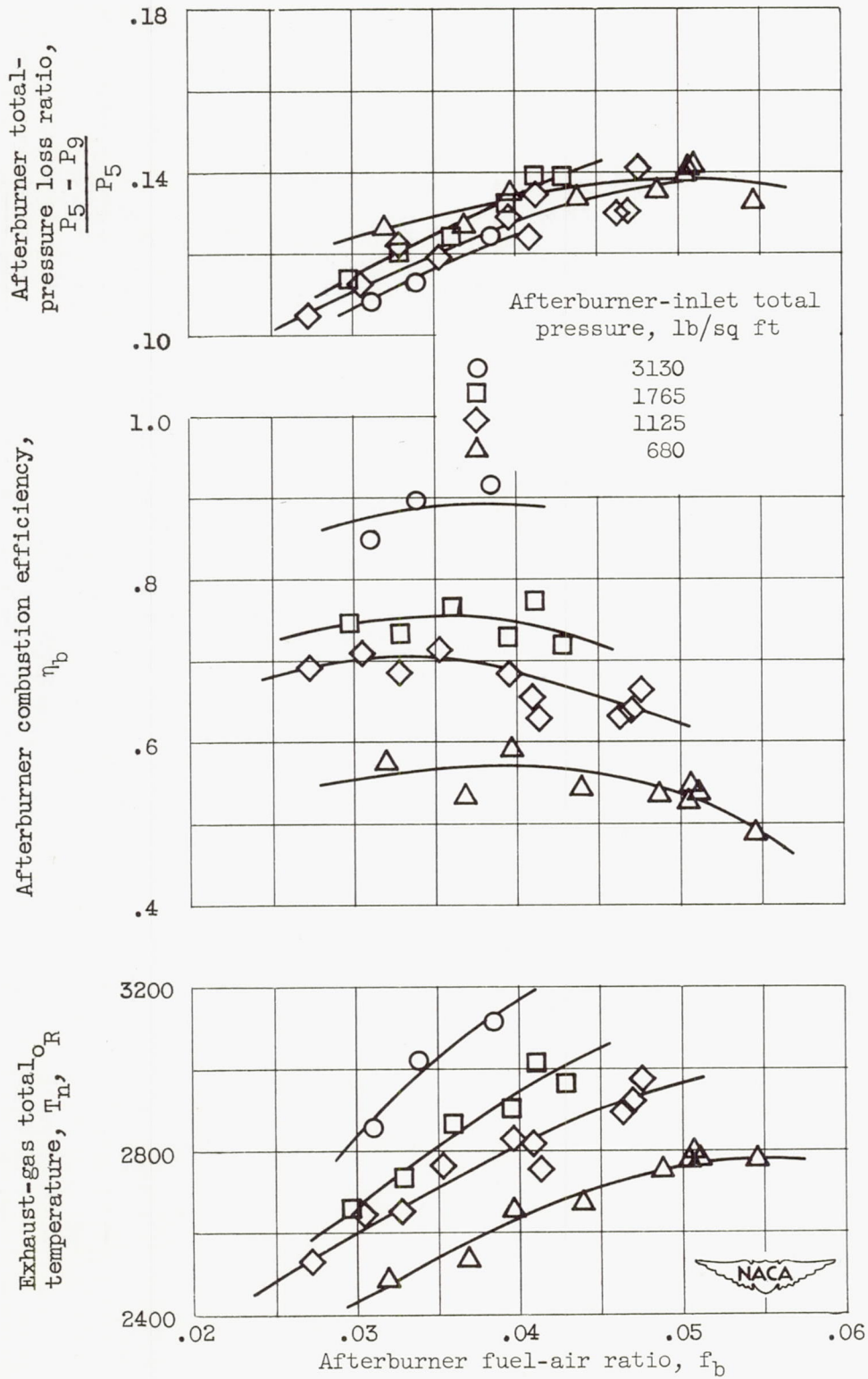


Figure 14. - Over-all performance of afterburner with flame holder 9. Afterburner-inlet temperature, 1810° R.

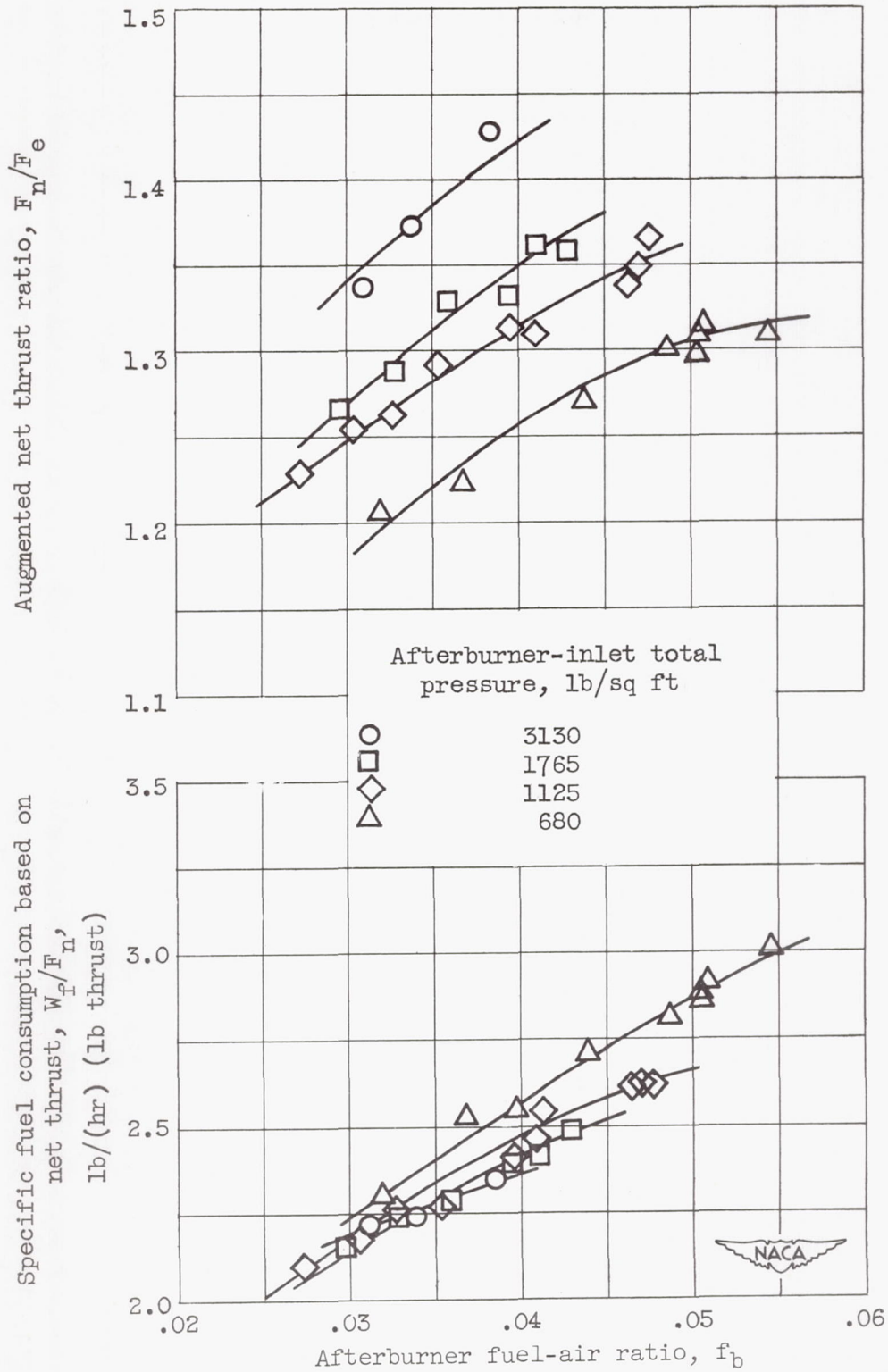
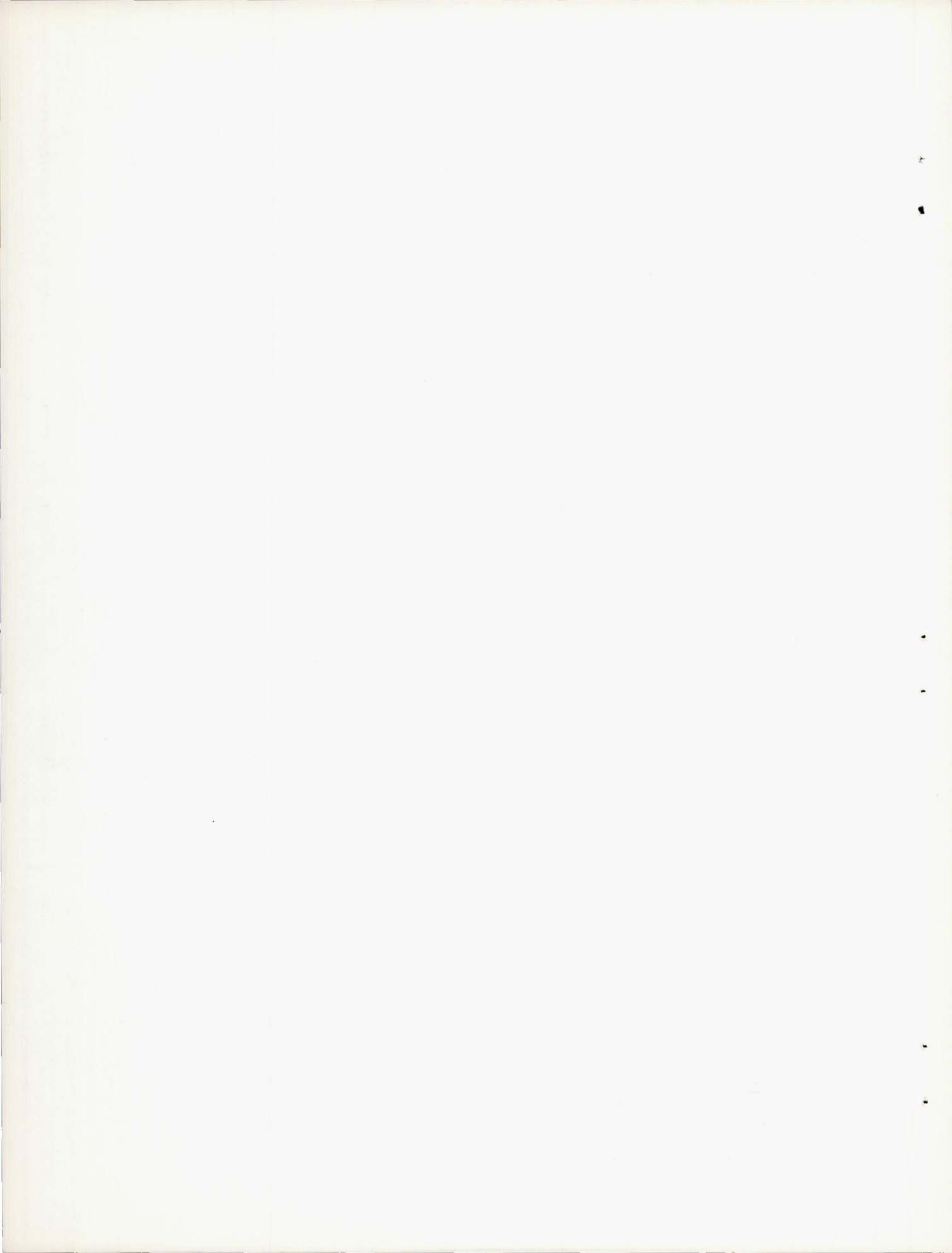
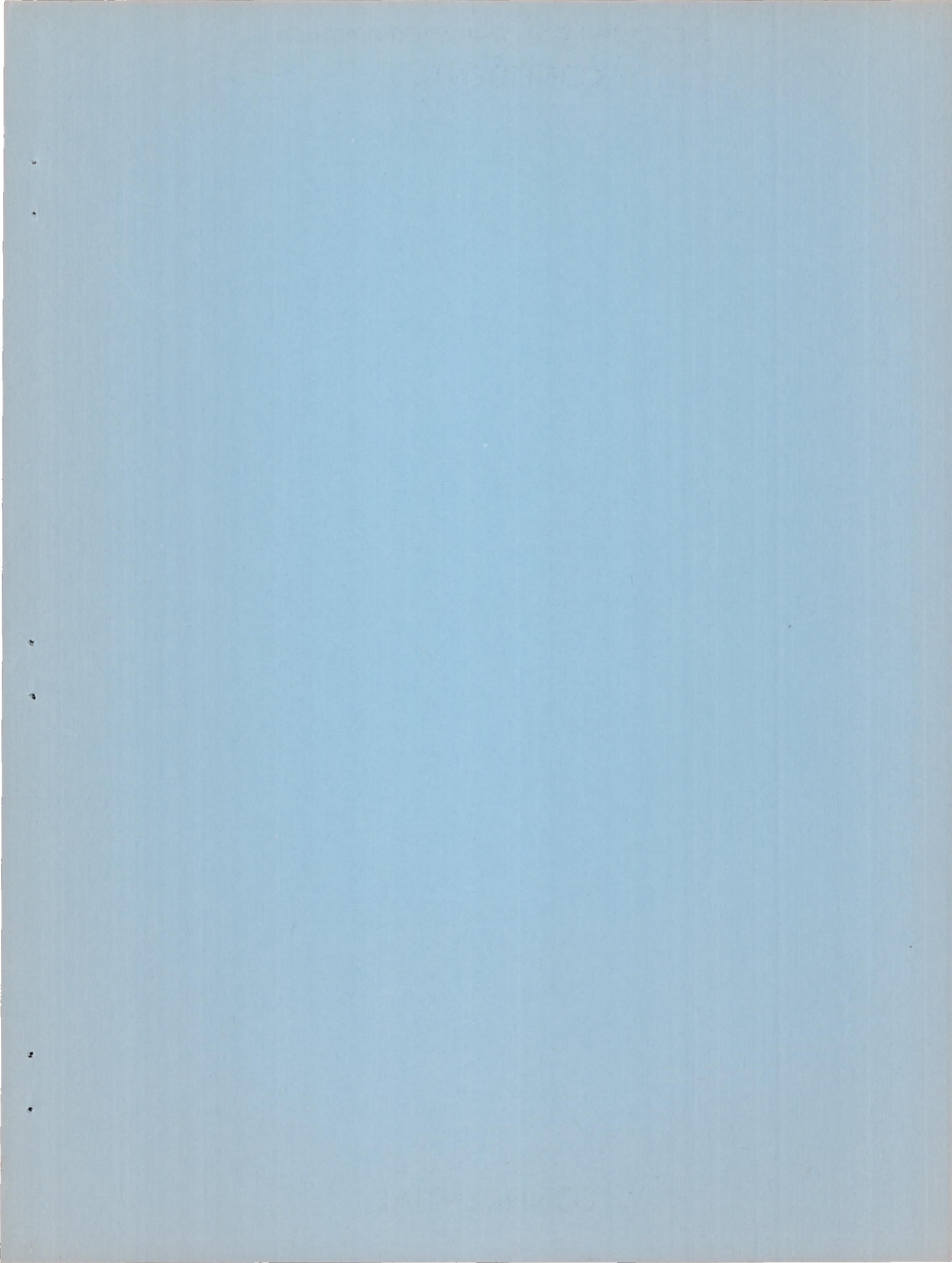


Figure 14. - Concluded. Over-all performance of afterburner with flame holder 9. Afterburner-inlet temperature, 1810° R.

3002





SECURITY INFORMATION
CONFIDENTIAL

CONFIDENTIAL